AĞRI İBRAHİM ÇEÇEN UNIVERSITY 2007

EASTERN ANATOLIAN JOURNAL OF SCIENCE 2015

EASTERN ANATOLIAN JOURNAL OF SCIENCE

VOLUME 8 - ISSUE 1

"THE LIGHT RISING FROM THE EAST"

2022

ISSN 2149-6137

Journal Name	**:** EASTERN ANATOLIAN JOURNAL OF SCIENCE
Managing Office	**:** Ağrı İbrahim Çeçen University
Web Site	**:** https://dergipark.org.tr/eajs
E-Mail	**:** eajs@agri.edu.tr
Managing Office Tel	**:** +90 472 215 50 82
Publication Language	**:** English
Publication Type	**:** International Journal
Online Published	**:** June, 2022

Owner on Behalf of Ağrı İbrahim Çeçen University

Prof. Dr. Abdulhalik KARABULUT

Rector

Editor-in-Chief

Prof. Dr. İbrahim HAN

ihan@agri.edu.tr

Associate Editor

Assist. Prof. Dr. Abdullah ÇAĞMAN

acagman@agri.edu.tr

PREFACE

Dear scientist,

I am happy to announce that Volume VIII - Issue I of the Eastern Anatolian Journal of Science (EAJS) has been published. This issue is composed of 4 research articles that possess some of the leading and advanced techniques of natural and applied sciences. On behalf of the owner of EAJS, I would like to thank all authors, referees, our editorial board members and section editors that provide valuable contributions for the publication of the issue.

EAJS will publish original and high-quality articles covering a wide range of topics in scientific research, dedicated to promoting high standards and excellence in the creation and dissemination of scientific knowledge. EAJS published in English is open access journal and abstracting and indexing by various international index services.

Authors are solicited to contribute to the EAJS by submitting articles that illustrate research results, projects, surveying works and industrial experiences that describe significant advances in the following areas, but are not limited to:

- Biology
- Chemistry
- Engineering
- Mathematics
- Nanoscience and Nanotechnology
- Physics

Our previous issues have an attraction in terms of scientific quality and impact factor of articles by favorable feedbacks of readers. Our editorial team lend wings to be an internationally reputable and pioneer journal of science by their outstanding scientific personality. I am hoping to work effectively with our editorial team in the future.

I'd like to express my gratitude to all authors, members of editorial board and contributing reviewers. My sincere thanks go to Prof. Dr. Abdulhalik KARABULUT, the rector of Ağrı İbrahim Çeçen University, sets the goal of being also a top-ranking university in scientific sense, for supporting and motivating us in every respect. I express my gratitude to the members of technical staff of the journal for the design and proofreading of the articles. Last but not least, my special thanks go to the respectable businessman Mr. İbrahim ÇEÇEN who unsparingly supports our university financially and emotionally, to his team and to the director and staff of IC foundation.

I invite scientists from all branches of science to contribute our journal by sending papers for publication in EAJS.

Prof. Dr. İbrahim HAN

Editor-in-Chief

CONTENTS

Conformal bi-slant Riemannian maps

Şener YANAN[1*]

[1] *Adıyaman University, Faculty of Arts and Science, Department of Mathematics, Adıyaman, Turkey,*
syanan@adiyaman.edu.tr

Abstract

In this study, conformal bi-slant Riemannian maps from an almost Hermitian manifold to a Riemannian manifold are defined. Integrability conditions of certain distributions on total manifolds are examined. Also, we studied that under which conditions, the distributions can define a totally geodesic foliation.

Keywords: Riemannian map, Conformal Riemannian map, Conformal bi-slant Riemannian map.

1. *Introduction*

At first, the notion of submersion was introduced by O'Neill (O'Neill 1966) and Gray (Gray 1967). Submersions between almost Hermitian manifolds were studied by Watson (Watson 1976). Then, this notion was studied in various types and generalized to Riemannian maps by Fischer (Fischer 1992). Riemannian maps between Riemannian manifolds are generalization of isometric immersions and Riemannian submersions. Let $\Phi\colon (\mathrm{M}_1, \mathrm{g}_1) \to (\mathrm{M}_2, \mathrm{g}_2)$ be a smooth map between Riemannian manifolds such that $0 < rank\Phi < min\{dim(M_1), dim(M_2)\}$. Then, the tangent bundle of TM_1 of M_1 has the following decomposition:

$$TM_1 = ker\Phi_* \oplus (ker\Phi_*)^{\perp}.$$

Since $rank\Phi < min\{dim(M_1), dim(M_2)\}$, we have $(range\Phi_*)^{\perp}$. Therefore, tangent bundle of TM_2 of M_2 has the following decomposition:

$$TM_2 = range\Phi_* \oplus (range\Phi_*)^{\perp}.$$

A smooth map $\Phi\colon (\mathrm{M}_1^m, \mathrm{g}_1) \to (\mathrm{M}_2^m, \mathrm{g}_2)$ is called Riemannian map at $p_1 \in M_1$ if the horizontal restriction $\Phi^h_{*p_1}\colon \left(ker\Phi_{*p_1}\right)^{\perp} \longrightarrow (range\Phi_*)$ is a linear isometry. Hence the Riemannian map satisfies the equation

$$g_1(X,Y) = g_2\left(\Phi_*(X), \Phi_*(Y)\right)$$

for $X, Y \in \Gamma((ker\Phi_*)^{\perp})$. So that isometric immersions and Riemannian submersions are particular Riemannian maps, respectively, with $\ker\Phi_* = \{0\}$ and $(\mathrm{range}\Phi_*)^{\perp} = \{0\}$ (Fischer 1992). Moreover, Şahin and Yanan searched conformal Riemannian maps (Şahin and Yanan 2018), (Şahin and Yanan 2019), (Yanan and Şahin 2022), see also (Yanan 2021). We say that $\Phi\colon (\mathrm{M}^{\mathrm{m}}, \mathrm{g}_{\mathrm{M}}) \longrightarrow (\mathrm{N}^{\mathrm{n}}, \mathrm{g}_{\mathrm{N}})$ is a conformal Riemannian map at $p \in M$ if $0 < rank\Phi_{*p} \leq min\{m, n\}$ and Φ_* maps the horizontal space $\left(\ker\left(\Phi_{*\mathrm{p}}\right)^{\perp}\right)$ conformally onto $range\left(\Phi_{*p}\right)$, i.e., there exist a number $\lambda^2(\mathrm{p}) \neq 0$ such that

$$g_N\left(\Phi_{*p}(X), \Phi_{*p}(Y)\right) = \lambda^2(p) g_M(X,Y)$$

for $X, Y \in \Gamma((ker\Phi_*)^{\perp})$. Also, Φ is called conformal Riemannian if Φ is conformal Riemannian at each $p \in M$. Here, λ is the dilation of Φ at a point $p \in M$ and it is a continuous function as $\lambda\colon M \to [0, \infty)$ (Şahin 2010), (Şahin 2017). If anyone wants to have more knowledge on submersion theory and bi-slant structure, the studies written by Aykurt Sepet could be seen (Akyol and Şahin 2019, Aykurt Sepet 2020), (Aykurt Sepet 2021).

An even-dimensional Riemannian manifold (M, g_M, J) is called an almost Hermitian manifold if there exists a tensor field J of type $(1,1)$ on M such that $J^2 = -I$ where I denotes the identity transformation of TM and

$$g_M(X,Y) = g_M(JX, JY), \forall X, Y \in \Gamma(TM).$$

Let (M, g_M, J) be an almost Hermitian manifold and its Levi-Civita connection ∇ with respect to g_M. If J is parallel with respect to ∇, i.e.

$$(\nabla_X J)Y = 0,$$

Received:17.02.2022
Accepted:12.04.2022
Published:30.06.2022
[*]*Corresponding author:* Şener YANAN, *PhD*
Adıyaman University, Faculty of Arts and Science, Department of Mathematics, Adıyaman Turkey
E-mail: syanan@adiyaman.edu.tr
Cite this article as: Ş. Yanan, Conformal Bi-slant Riemannian Maps, *Eastern Anatolian Journal of Science, Vol. 8, Issue 1, 1-8, 2022.*

we say M is a Kaehler manifold (Yano and Kon 1984).

Therefore, we define conformal bi-slant Riemannian maps from an almost Hermitian manifold to a Riemannian manifold as a generalization of conformal anti-invariant Riemannian maps (Şahin and Yanan 2018), conformal semi-invariant Riemannian maps (Şahin and Yanan 2019), conformal semi-slant Riemannian maps (Yanan 2022b) and conformal hemi-slant Riemannian maps (Yanan 2022a). Also, an explicit example is given. Some geometric properties of this type maps are examined.

2. Materials and Methods

In this section, we give several definitions and results to be used along the study for conformal bi-slant Riemannian maps. Let $\Phi: (M, g_M) \longrightarrow (N, g_N)$ be a smooth map between Riemannian manifolds. The second fundamental form of Φ is defined by

$$(\nabla\Phi_*)(X,Y) = \nabla^{\Phi}_X \Phi_*(Y) - \Phi_*(\nabla_X Y)$$

for $X, Y \in \Gamma(TM)$. The second fundamental form $(\nabla\Phi_*)$ is symmetric. Note that Φ is said to be totally geodesic map if $(\nabla F_*)(X,Y) = 0$ for all $X, Y \in \Gamma(TM)$ (Nore 1986). Here, we define O'Neill's tensor fields $\mathcal{T}$ and $\mathcal{A}$ as

$$\mathcal{A}_X Y = h\nabla_{hX} vY + v\nabla_{hX} hY,$$
$$\mathcal{T}_X Y = h\nabla_{vX} vY + v\nabla_{vX} hY,$$

for $X, Y \in \Gamma(TM)$ with the Levi-Civita connection ∇ of g_M. Here, we denote by v and h the projections on the vertical distribution $ker\Phi_*$ and the horizontal distribution $(ker\Phi_*)^{\perp}$, respectively. For any $X \in \Gamma(TM)$, $\mathcal{T}_X$ and $\mathcal{A}_X$ are skew-symmetric operators on $(\Gamma(TM), g)$ reversing the horizontal and the vertical distributions. Also, $\mathcal{T}$ is vertical, $\mathcal{T}_X = \mathcal{T}_{vX}$ and $\mathcal{A}$ is horizontal, $\mathcal{A}_X = \mathcal{A}_{hX}$. Note that the tensor field $\mathcal{T}$ is symmetric on the vertical distribution (O'Neill 1966). In addition, by definitions of O'Neill's tensor fields, we have

$$\nabla_U V = \mathcal{T}_U V + v\nabla_U V,$$
$$\nabla_U X = h\nabla_U X + \mathcal{T}_U X,$$
$$\nabla_X V = \mathcal{A}_X V + v\nabla_X V,$$
$$\nabla_X Y = h\nabla_X Y + \mathcal{A}_X Y$$

for $X, Y \in \Gamma((ker\Phi_*)^{\perp})$ and $U, V \in \Gamma(ker\Phi_*)$ (Falcitelli et al. 2004).

If a vector field X on M is related to a vector field X' on N, we say X is a projectable vector field. If X is both a horizontal and a projectable vector field, we say X is a basic vector field on M (Baird and Wood 2003). Throughout this study, when we mention a horizontal vector field, we always consider a basic vector field.

On the other hand, let $\Phi: (M^m, g_M) \longrightarrow (N^n, g_N)$ be a conformal Riemannian map between Riemannian manifolds. Then, we have

$$(\nabla\Phi_*)(X,Y)\,|_{range\Phi_*} = X(\ln\lambda)\Phi_*(Y) + Y(\ln\lambda)\Phi_*(X) - g_M(X,Y)\Phi_*\big(grad(\ln\lambda)\big)$$

where $X, Y \in \Gamma((ker\Phi_*)^{\perp})$ (Şahin 2010). Hence, we obtain $\nabla^{\Phi}_X \Phi_*(Y)$ as

$$\nabla^{\Phi}_X \Phi_*(Y) = \Phi_*(h\nabla_X Y) + X(\ln\lambda)\Phi_*(Y) + Y(\ln\lambda)\Phi_*(X) - g_M(X,Y)\Phi_*\big(grad(\ln\lambda)\big) + (\nabla\Phi_*)^{\perp}(X,Y)$$

where $(\nabla\Phi_*)^{\perp}(X,Y)$ is the component of $(\nabla\Phi_*)(X,Y)$ on $(range\Phi_*)^{\perp}$ for $X, Y \in \Gamma((ker\Phi_*)^{\perp})$ (Şahin and Yanan 2018).

3. Results

In this section, we define conformal bi-slant Riemannian maps and give an example. In addition, we present conditions to be integrable and to define totally geodesic foliation for distributions.

Definition 3.1. Let (M, g_M, J) be an almost Hermitian manifold and (N, g_N) be a Riemannian manifold. Then, a conformal Riemannian map $\Phi: (M, g_M, J) \longrightarrow (N, g_N)$ is called a conformal bi-slant Riemannian map if and only if D_1 and D_2 are slant distributions with their slant angles θ_1 and θ_2, respectively, such that

$$ker\Phi_* = D_1 \oplus D_2.$$

Here, if the slant angles satisfy that $\theta_1, \theta_2 \neq 0, \frac{\pi}{2}$, Φ is called a proper conformal bi-slant Riemannian map.

Therefore, suppose that the dimensions of D_1 and D_2 are m_1 and m_2, respectively. Then, we have the next notions.

i. If $m_1 = 0$ and $\theta_2 = \frac{\pi}{2}$, then Φ is a conformal anti-invariant Riemannian map (Şahin and Yanan 2018),

ii. If $m_1, m_2 \neq 0$, $\theta_1 = 0$ and $\theta_2 = \frac{\pi}{2}$, then Φ is a conformal semi-invariant Riemannian map (Şahin and Yanan 2019),

iii. If $m_1, m_2 \neq 0$, $\theta_1 = 0$ and $0 < \theta_2 < \frac{\pi}{2}$, then then Φ is a conformal semi-slant Riemannian map (Yanan 2022b),

iv. If $m_1, m_2 \neq 0$, $\theta_1 = \frac{\pi}{2}$ and $0 < \theta_2 < \frac{\pi}{2}$, then then Φ is a conformal hemi-slant Riemannian map (Yanan 2022a).

After these cases, we give an explicit example for proper conformal bi-slant Riemannian map.

Example 3.2. Let Φ be a map defined as

$$\Phi: R^8 \longrightarrow R^5: e^2\left(\frac{x_1 - x_7}{\sqrt{2}}, x_4, \frac{x_5 - x_6}{\sqrt{2}}, x_2, \gamma\right)$$

where γ is the real number. The almost complex structure J_β on R^8 is

$$J_\beta = (cos\,\beta)J_1 + (sin\,\beta)J_2, 0 < \beta \leq \frac{\pi}{2}$$

where

$$J_1 = (-a_2, a_1, -a_4, a_3, -a_6, a_5, -a_8, a_7)$$

and

$$J_2 = (-a_8, -a_7, -a_6, -a_5, a_4, a_3, a_2, a_1).$$

Then, we have the horizontal distribution as

$$(ker\Phi_*)^\perp = \{X_1 = \frac{e^2}{\sqrt{2}}\left(\frac{\partial}{\partial x_1} - \frac{\partial}{\partial x_7}\right), X_2 = e^2\frac{\partial}{\partial x_4},$$

$$X_3 = \frac{e^2}{\sqrt{2}}\left(\frac{\partial}{\partial x_5} - \frac{\partial}{\partial x_6}\right), X_4 = e^2\frac{\partial}{\partial x_2}\}$$

and the vertical distribution as

$$ker\Phi_* = \{U_1 = \frac{1}{\sqrt{2}}\left(\frac{\partial}{\partial x_1} + \frac{\partial}{\partial x_7}\right), U_2 = \frac{\partial}{\partial x_3},$$

$$U_3 = \frac{1}{\sqrt{2}}\left(\frac{\partial}{\partial x_5} + \frac{\partial}{\partial x_6}\right), X_4 = \frac{\partial}{\partial x_8}\}.$$

Here, we say Φ is a conformal Riemannian map with $\lambda = e^2$ *and* $rank\Phi_* = 4$. Then, by some calculations we obtain the slant distributions as $D_1 = \{U_1, U_2\}$ and $D_2 = \{U_3, U_4\}$. Hence, Φ is a proper conformal bi-slant Riemannian map with respect to the slant distributions

$$D_1 = \{U_1, U_2\}, D_2 = \{U_3, U_4\}$$

and the slant angles

$$cos\,\theta_1 = \frac{1}{\sqrt{2}}(cos\,\beta + sin\,\beta),\ cos\,\theta_2 = \frac{1}{\sqrt{2}}sin\,\beta.$$

Now, we explain decomposition of distributions for a conformal bi-slant Riemannian map.

Assume that Φ be a conformal bi-slant Riemannian map from an almost Hermitian manifold (M, g_M, J) to a Riemannian manifold (N, g_N). For any $U \in \Gamma(ker\Phi_*)$, we have

$$U = PU + QU,$$

where $PU \in \Gamma(D_1)$ and $QU \in \Gamma(D_2)$. On the other hand, we have

$$JU = \psi U + \phi U,$$

for $U \in \Gamma(ker\Phi_*)$ where $\phi U \in \Gamma((ker\Phi_*)^\perp)$ and $\psi U \in \Gamma(ker\Phi_*)$. Also, for any $X \in \Gamma((ker\Phi_*)^\perp)$, we write

$$JX = BX + CX,$$

where $BX \in \Gamma(ker\Phi_*)$ and $CX \in \Gamma((ker\Phi_*)^\perp)$. Therefore, the horizontal distribution $(ker\Phi_*)^\perp$ can be decomposed as

$$(ker\Phi_*)^\perp = \phi D_1 \oplus \phi D_2 \oplus \mu,$$

where μ is the orthogonal complementary distribution of $\phi D_1 \oplus \phi D_2$ in $(ker\Phi_*)^\perp$.

We have the following theorem same for conformal bi-slant Riemannian maps (Aykurt Sepet 2021).

Theorem 3.3. Let Φ be a conformal bi-slant Riemannian map from an almost Hermitian manifold (M, g_M, J) to a Riemannian manifold (N, g_N) with slant angles θ_1 and θ_2. Then, we have

$$\psi^2 U_i = -(cos^2\,\theta_i)U_i$$

for $U_i \in \Gamma(D_i)$, $i = 1,2$.

After then, we examine integrability conditions for certain distributions.

Theorem 3.4. Let Φ be a proper conformal bi-slant Riemannian map from a Kaehler manifold (M, g_M, J) to a Riemannian manifold (N, g_N) with slant angles θ_1 and θ_2. Then, the distribution D_1 is integrable if and only if

$$g_N\left((\nabla\Phi_*)(V_1, U_2), \Phi_*\left(\phi(JU_1)\right)\right)$$

$$= \lambda^2\,cos^2\,\theta_1\,g_M\left(v\nabla_{V_1}U_1, U_2\right)$$

$$-g_M\left(v\nabla_{U_1}V_1 + v\nabla_{V_1}\psi\phi U_1, U_2\right)$$

for $U_1, V_1 \in \Gamma(D_1)$ and $U_2 \in \Gamma(D_2)$.

Proof. Since the vertical distribution $ker\Phi_*$ is always integrable, we only examine $0 = g_M([U_1,V_1],U_2)$ for $U_1,V_1 \in \Gamma(D_1)$ and $U_2 \in \Gamma(D_2)$. To get this equality, we write

$$\begin{aligned}[U_1,V_1] &= \nabla_{U_1}V_1 - \nabla_{V_1}U_1 \\ &= v\nabla_{U_1}V_1 - \nabla_{V_1}\psi^2U_1 + \nabla_{V_1}\phi\psi U_1 \\ &\quad +\nabla_{V_1}\psi\phi U_1 \\ &= v\nabla_{U_1}V_1 - cos^2\,\theta_1\nabla_{V_1}U_1 + h\nabla_{V_1}\phi\psi U_1 \\ &\quad +\mathcal{T}_{V_1}\phi\psi U_1 + h\nabla_{V_1}\phi^2U_1 + \mathcal{T}_{V_1}\phi^2U_1 \\ &\quad +\mathcal{T}_{V_1}\psi\phi U_1 + v\nabla_{V_1}\psi\phi U_1.\end{aligned}$$

Now, for $U_2 \in \Gamma(D_2)$, we get

$$\begin{aligned}g_M([U_1,V_1],U_2) &= g_M\big(v\nabla_{U_1}V_1 - cos^2\,\theta_1\nabla_{V_1}U_1\,,U_2\big) \\ &\quad +g_M\big(\mathcal{T}_{V_1}\phi(JU_1) + v\nabla_{V_1}\psi\phi U_1,U_2\big).\end{aligned}$$

Since $\mathcal{T}$ is an anti-symmetric tensor field with respect to g_M, we have

$$g_M\big(\mathcal{T}_{V_1}\phi(JU_1),U_2\big) = -g_M\left(\mathcal{T}_{V_1}U_2,\phi(JU_1)\right).$$

Then, since the map Φ is conformal by using definition of second fundamental form of the map, we get

$$\begin{aligned}&-g_M\left(\mathcal{T}_{V_1}U_2,\phi(JU_1)\right) \\ &\qquad = \tfrac{1}{\lambda^2}g_N\left((\nabla\Phi_*)(V_1,U_2),\Phi_*\big(\phi(JU_1)\big)\right).\end{aligned}$$

At last, we obtain

$$\begin{aligned}&g_M([U_1,V_1],U_2) \\ &\qquad = -cos^2\,\theta_1 g_M\big(v\nabla_{V_1}U_1,U_2\big) \\ &\qquad\quad +g_M\big(v\nabla_{U_1}V_1 + v\nabla_{V_1}\psi\phi U_1,U_2\big) \\ &\qquad\quad +\tfrac{1}{\lambda^2}g_N\left((\nabla\Phi_*)(V_1,U_2),\Phi_*\big(\phi(JU_1)\big)\right).\end{aligned}$$

The proof is complete.

Theorem 3.5. Let Φ be a proper conformal bi-slant Riemannian map from a Kaehler manifold (M,g_M,J) to a Riemannian manifold (N,g_N) with slant angles θ_1 and θ_2. Then, the distribution D_2 is integrable if and only if

$$\begin{aligned}&g_N\left((\nabla\Phi_*)(V_2,U_1),\Phi_*\big(\phi(JU_2)\big)\right) \\ &\qquad = \lambda^2\,cos^2\,\theta_2\,g_M\big(v\nabla_{V_2}U_2,U_1\big) \\ &\qquad\quad -g_M\big(v\nabla_{U_2}V_2 + v\nabla_{V_2}\psi\phi U_2,U_1\big)\end{aligned}$$

for $U_2,V_2 \in \Gamma(D_2)$ and $U_1 \in \Gamma(D_1)$.

Proof. The proof of the Theorem 3.5. can be done in a similar way as Theorem 3.4.

Theorem 3.6. Let Φ be a proper conformal bi-slant Riemannian map from a Kaehler manifold (M,g_M,J) to a Riemannian manifold (N,g_N) with slant angles θ_1 and θ_2. Then, the distribution D_1 defines a totally geodesic foliation on M if and only if

i. $$\begin{aligned}&g_N\big((\nabla\Phi_*)(U_1,\psi V_1),\Phi_*(\phi U_2)\big) - \\ &\quad g_N\big((\nabla\Phi_*)(U_1,V_1),\Phi_*(\phi\psi U_2)\big) \\ &\qquad = -\lambda^2\,cos^2\,\theta_2\,g_M\big(v\nabla_{U_1}U_2,V_1\big) \\ &\qquad\quad -\lambda^2 g_M\big(h\nabla_{U_1}\phi U_2,\phi V_1\big)\end{aligned}$$

ii. $$\begin{aligned}&g_N\big((\nabla\Phi_*)(U_1,BX),\Phi_*(\phi V_1)\big) \\ &\qquad = \lambda^2 g_M\big(h\nabla_{U_1}\phi\psi V_1,X\big) \\ &\qquad\quad +\lambda^2 g_M\big(h\nabla_{U_1}\phi V_1,CX\big)\end{aligned}$$

for $U_1,V_1 \in \Gamma(D_1)$, $U_2 \in \Gamma(D_2)$ and $X \in \Gamma((ker\Phi_*)^\perp)$.

Proof. If the distribution D_1 defines a totally geodesic foliation on M, we have $0 = g_M\big(\nabla_{U_1}V_1,U_2\big)$ and $0 = g_M\big(\nabla_{U_1}V_1,X\big)$ for $U_1,V_1 \in \Gamma(D_1)$, $U_2 \in \Gamma(D_2)$ and $X \in \Gamma((ker\Phi_*)^\perp)$. At first, we get

$$\begin{aligned}g_M\big(\nabla_{U_1}V_1,U_2\big) &= g_M\big(\nabla_{U_1}\psi^2U_2,V_1\big) \\ &\quad + g_M\big(\nabla_{U_1}\phi\psi U_2,V_1\big) \\ &\quad +g_M\big(\mathcal{T}_{\mathcal{U}_1}\psi V_1,\phi U_2\big) \\ &\quad -g_M\big(h\nabla_{U_1}\phi U_2,\phi V_1\big)\end{aligned}$$

for $U_1,V_1 \in \Gamma(D_1)$ and $U_2 \in \Gamma(D_2)$. On the other hand, we have from definition of the second fundamental form of the map Φ and $\mathcal{T}$ is an anti-symmetric tensor field with respect to g_M

$$\begin{aligned}&g_M\big(\mathcal{T}_{\mathcal{U}_1}\phi\psi U_2,V_1\big) \\ &\qquad = -g_M(\mathcal{T}_{\mathcal{U}_1}\mathcal{V}_1,\phi\psi\mathcal{U}_2) \\ &\qquad = \tfrac{1}{\lambda^2}g_N\big((\nabla\Phi_*)(U_1,V_1),\Phi_*(\phi\psi\mathcal{U}_2)\big)\end{aligned}$$

and

$$\begin{aligned}&g_M\big(\mathcal{T}_{\mathcal{U}_1}\psi V_1,\phi U_2\big) \\ &\qquad = -\tfrac{1}{\lambda^2}g_N\big((\nabla\Phi_*)(U_1,\psi V_1),\Phi_*(\phi\mathcal{U}_2)\big).\end{aligned}$$

By using these equalities and from Theorem 3.3., we obtain

$$\begin{aligned}g_M\big(\nabla_{U_1}V_1,U_2\big) &= -cos^2\,\theta_2\,g_M\big(v\nabla_{U_1}U_2,V_1\big) \\ &\quad -g_M\big(h\nabla_{U_1}\phi U_2,\phi V_1\big) \\ &\quad +\tfrac{1}{\lambda^2}g_N\big((\nabla\Phi_*)(U_1,V_1),\Phi_*(\phi\psi\mathcal{U}_2)\big) \\ &\quad -\tfrac{1}{\lambda^2}g_N\big((\nabla\Phi_*)(U_1,\psi V_1),\Phi_*(\phi\mathcal{U}_2)\big).\end{aligned}$$

From last equation, we have the proof of i. Now, we examine $0 = g_M\big(\nabla_{U_1}V_1,X\big)$ for $U_1,V_1 \in \Gamma(D_1)$ and $X \in \Gamma((ker\Phi_*)^\perp)$. By some similar computations, we have

$$\begin{aligned}g_M\big(\nabla_{U_1}V_1,X\big) &= cos^2\,\theta_1\,g_M\big(\nabla_{U_1}V_1,X\big) \\ &\quad -g_M\big(h\nabla_{U_1}\phi\psi V_1,X\big) \\ &\quad +g_M\big(\mathcal{T}_{\mathcal{U}_1}\phi V_1,BX\big) \\ &\quad -g_M\big(h\nabla_{U_1}\phi V_1,CX\big)\end{aligned}$$

$$sin^2\,\theta_1\, g_M(\nabla_{U_1}V_1,X) = -g_M(h\nabla_{U_1}\phi\psi V_1,X) - g_M(h\nabla_{U_1}\phi V_1,CX) - g_M(\mathcal{T}_{U_1}BX,\phi V_1)$$

$$sin^2\,\theta_1\, g_M(\nabla_{U_1}V_1,X) = -g_M(h\nabla_{U_1}\phi\psi V_1,X) - g_M(h\nabla_{U_1}\phi V_1,CX) + \tfrac{1}{\lambda^2}g_N\big((\nabla\Phi_*)(U_1,BX),\Phi_*(\phi V_1)\big).$$

From the last equation, we obtain ii. Hence, the proof of Theorem 3.6. is complete.

Theorem 3.7. Let Φ be a proper conformal bi-slant Riemannian map from a Kaehler manifold (M,g_M,J) to a Riemannian manifold (N,g_N) with slant angles θ_1 and θ_2. Then, the distribution D_2 defines a totally geodesic foliation on M if and only if

i. $$g_N\big((\nabla\Phi_*)(U_2,\psi U_1),\Phi_*(\phi V_2)\big) - g_N\big((\nabla\Phi_*)(U_2,U_1),\Phi_*(\phi\psi V_2)\big) = \lambda^2 g_M\big(h\nabla_{U_2}\phi V_2,\phi U_1\big)$$

ii. $$g_N\big((\nabla\Phi_*)(U_2,BX),\Phi_*(\phi V_2)\big) = \lambda^2 g_M\big(h\nabla_{U_2}\phi V_2,CX\big) - \lambda^2 g_M\big(h\nabla_{U_2}\phi\psi V_2,X\big)$$

for $U_1\in\Gamma(D_1)$, $U_2,V_2\in\Gamma(D_2)$ and $X\in\Gamma((ker\Phi_*)^{\perp})$.

Proof. Here, we search $0=g_M\big(\nabla_{U_2}V_2,U_1\big)$ and $0=g_M\big(\nabla_{U_2}V_2,X\big)$ to get conditions i. and ii. for $U_1\in\Gamma(D_1)$, $U_2,V_2\in\Gamma(D_2)$ and $X\in\Gamma((ker\Phi_*)^{\perp})$. Firstly, we have

$$g_M\big(\nabla_{U_2}V_2,U_1\big) = cos^2\,\theta_2\, g_M\big(\nabla_{U_2}V_2,U_1\big) - g_M\big(\nabla_{U_2}\phi\psi V_2,U_1\big) + g_M\big(\mathcal{T}_{U_2}\phi V_2,\psi U_1\big) + g_M\big(h\nabla_{U_2}\phi V_2,\phi U_1\big)$$

for $U_1\in\Gamma(D_1)$ and $U_2,V_2\in\Gamma(D_2)$. By using anti-symmetry property of $\mathcal{T}$ and from Theorem 3.3., we get

$$sin^2\,\theta_2\, g_M\big(\nabla_{U_2}V_2,U_1\big) = g_M\big(\mathcal{T}_{U_2}U_1,\phi\psi U_1\big) - g_M\big(\mathcal{T}_{U_2}\psi U_1,\phi V_2\big) + g_M\big(h\nabla_{U_2}\phi V_2,\phi U_1\big).$$

Since the map Φ is conformal, we obtain

$$sin^2\,\theta_2\, g_M\big(\nabla_{U_2}V_2,U_1\big) = g_M\big(h\nabla_{U_2}\phi V_2,\phi U_1\big) - \tfrac{1}{\lambda^2}g_N\big((\nabla\Phi_*)(U_2,\psi U_1),\Phi_*(\phi V_2)\big) + \tfrac{1}{\lambda^2}g_N\big((\nabla\Phi_*)(U_2,U_1),\Phi_*(\phi\psi V_2)\big).$$

From the last equation, we have the proof of i. Now, we examine $0=g_M\big(\nabla_{U_2}V_2,X\big)$ for $U_2,V_2\in\Gamma(D_2)$ and $X\in\Gamma((ker\Phi_*)^{\perp})$. By similar calculations, we have

$$g_M\big(\nabla_{U_2}V_2,X\big) = cos^2\,\theta_2\, g_M\big(\nabla_{U_2}V_2,X\big) - g_M\big(h\nabla_{U_2}\phi\psi V_2,X\big) - g_M\big(\mathcal{T}_{U_2}BX,\phi V_2\big) + g_M\big(h\nabla_{U_2}\phi V_2,CX\big)$$

for $U_2,V_2\in\Gamma(D_2)$ and $X\in\Gamma((ker\Phi_*)^{\perp})$. At last, from conformality of the map, we obtain

$$sin^2\,\theta_2\, g_M\big(\nabla_{U_2}V_2,X\big) = g_M\big(h\nabla_{U_2}\phi V_2,CX\big) - g_M\big(h\nabla_{U_2}\phi\psi V_2,X\big) - \tfrac{1}{\lambda^2}g_N\big((\nabla\Phi_*)(U_2,BX),\Phi_*(\phi V_2)\big).$$

Hence, we have the proof of ii. clearly.

Theorem 3.8. Let Φ be a proper conformal bi-slant Riemannian map from a Kaehler manifold (M,g_M,J) to a Riemannian manifold (N,g_N) with slant angles θ_1 and θ_2. Then the vertical distribution $ker\Phi_*$ is a locally product as $M_{D_1}\times M_{D_2}$ if and only if the equations in Theorem 3.6. and Theorem 3.7. are hold where M_{D_1} and M_{D_2} are integral manifolds of the distributions D_1 and D_2, respectively.

Theorem 3.9. Let Φ be a proper conformal bi-slant Riemannian map from a Kaehler manifold (M,g_M,J) to a Riemannian manifold (N,g_N) with slant angles θ_1 and θ_2. Then, the distribution $(ker\Phi_*)^{\perp}$ defines a totally geodesic foliation on M if and only if

$$\begin{aligned}\lambda^2\{&X(ln\,\lambda)g_M(CY,\phi U_i)+CY(ln\,\lambda)g_M(X,\phi U_i)\\&-\phi U_i(ln\,\lambda)g_M(X,CY)\\&-X(ln\,\lambda)g_M(Y,\phi\psi U_i)\\&-Y(ln\,\lambda)g_M(X,\phi\psi U_i)\\&+\phi\psi U_i(ln\,\lambda)g_M(X,Y)\}\\=\;&g_N\Big((\nabla\Phi_*)(X,BY)+\nabla^{\Phi}_X\Phi_*(CY),\Phi_*(\phi U_i)\Big)\\&-g_N\Big(\nabla^{\Phi}_X\Phi_*(Y),\Phi_*(\phi\psi U_i)\Big),\qquad i=1,2\end{aligned}$$

for $X,Y\in\Gamma((ker\Phi_*)^{\perp})$, $U_1\in\Gamma(D_1)$ and $U_2\in\Gamma(D_2)$.

Proof. Since Φ is a proper conformal bi-slant Riemannian map, we have two orthogonal complement distribution that D_1 and D_2 in $ker\Phi_*$, respectively. So, we examine $0=g_M(\nabla_XY,U_1)$ and $0=g_M(\nabla_XY,U_2)$ for $X,Y\in\Gamma((ker\Phi_*)^{\perp})$, $U_1\in\Gamma(D_1)$ and $U_2\in\Gamma(D_2)$. Since we will use the same calculations for these two cases, we examine just one for U_1. Then, it will be same for U_2. Firstly, since M is a Kaehler manifold, we get

$$g_M(\nabla_XY,U_1) = g_M(\mathcal{A}_XBY,\phi U_1) + g_M(h\nabla_XCY,\phi U_1)$$

$$+cos^2\theta_1\, g_M(\nabla_X Y, U_1)$$
$$-g_M(h\nabla_X Y, \phi\psi U_1).$$

Since the map Φ is conformal Riemannian map, we obtain

$$\begin{aligned}
&sin^2\theta_1\, g_M(\nabla_X Y, U_1)\\
&= \tfrac{1}{\lambda^2} g_N\big((\nabla\Phi_*)(X,BY), \Phi_*(\phi U_1)\big)\\
&+\tfrac{1}{\lambda^2}\{g_N\left(\nabla^{\Phi}_X \Phi_*(CY), \Phi_*(\phi U_1)\right)\\
&-X(ln\,\lambda) g_N\big(\Phi_*(CY), \Phi_*(\phi U_1)\big)\\
&-CY(ln\,\lambda) g_N\big(\Phi_*(X), \Phi_*(\phi U_1)\big)\\
&+g_M(X, CY) g_N\left(\Phi_*\big(grad(ln\,\lambda)\big), \Phi_*(\phi U_1)\right)\}\\
&-\frac{1}{\lambda^2}\{g_N\left(\nabla^{\Phi}_X \Phi_*(Y), \Phi_*(\phi\psi U_1)\right)\\
&-X(ln\,\lambda) g_N\big(\Phi_*(Y), \Phi_*(\phi\psi U_1)\big)\\
&-Y(ln\,\lambda) g_N\big(\Phi_*(X), \Phi_*(\phi\psi U_1)\big)\\
&+g_M(X,Y) g_N\left(\Phi_*\big(grad(ln\,\lambda)\big), \Phi_*(\phi\psi U_1)\right)\}
\end{aligned}$$

$$\begin{aligned}
&sin^2\theta_1\, g_M(\nabla_X Y, U_1)\\
&= \tfrac{1}{\lambda^2} g_N\big((\nabla\Phi_*)(X,BY), \Phi_*(\phi U_1)\big)\\
&+\tfrac{1}{\lambda^2}\{g_N\left(\nabla^{\Phi}_X \Phi_*(CY), \Phi_*(\phi U_1)\right)\\
&-g_N\left(\nabla^{\Phi}_X \Phi_*(Y), \Phi_*(\phi\psi U_1)\right)\\
&-X(ln\,\lambda) g_M(CY, \phi U_1)\\
&-CY(ln\,\lambda) g_M(X, \phi U_1)\\
&+g_M(X, CY)\ \phi U_1(ln\,\lambda)\\
&+X(ln\,\lambda) g_M(Y, \phi\psi U_1)\\
&+Y(ln\,\lambda) g_M(X, \phi U_1)\\
&-g_M(X,Y)\ \phi\psi U_1(ln\,\lambda).
\end{aligned}$$

It is clear that the distribution $(ker\Phi_*)^{\perp}$ defines a totally geodesic foliation on M for $X, Y \in \Gamma((ker\Phi_*)^{\perp})$ and $U_1 \in \Gamma(D_1)$.

Theorem 3.10. Let Φ be a proper conformal bi-slant Riemannian map from a Kaehler manifold (M, g_M, J) to a Riemannian manifold (N, g_N) with slant angles θ_1 and θ_2. Then, the distribution $ker\Phi_*$ defines a totally geodesic foliation on M if and only if

$$\begin{aligned}
&g_N\big((\nabla\Phi_*)(\phi\psi V, U), \Phi_*(X)\big)\\
&= \lambda^2\, cos^2\theta_1\, g_M(\nabla_U PV, X)\\
&+\lambda^2\, cos^2\theta_2\, g_M(\nabla_U QV, X)\\
&+\lambda^2 g_M(\nabla_U \phi V, JX)
\end{aligned}$$

for $X \in \Gamma((ker\Phi_*)^{\perp})$ and $U, V \in \Gamma(ker\Phi_*)$.

Proof. Now, we examine $0 = g_M(\nabla_U V, X)$ to show that the distribution $ker\Phi_*$ defines a totally geodesic foliation on M. Hence, we get

$$\begin{aligned}
g_M(\nabla_U V, X) &= -g_M(\nabla_U J\psi PV, X)\\
&+g_M(h\nabla_U \phi PV + \mathcal{T}_{\mathcal{U}}\phi PV, BX + CX)\\
&-g_M(\nabla_U J\psi QV, X)\\
&+g_M(h\nabla_U \phi QV + \mathcal{T}_{\mathcal{U}}\phi QV, BX + CX)\\
g_M(\nabla_U V, X) &= -g_M(\nabla_U \psi^2 PV + \nabla_U \phi\psi PV, X)\\
&- g_M(\nabla_U \psi^2 QV + \nabla_U \phi\psi QV, X)\\
&+ g_M(h\nabla_U \phi PV + h\nabla_U \phi QV, CX)\\
&+ g_M(\mathcal{T}_{\mathcal{U}}\phi PV + \mathcal{T}_{\mathcal{U}}\phi QV, BX)\\
g_M(\nabla_U V, X) &= cos^2\theta_1\, g_M(\nabla_U PV, X)\\
&- g_M(h\nabla_U \phi\psi PV, X)\\
&+ cos^2\theta_2\, g_M(\nabla_U QV, X)\\
&- g_M(h\nabla_U \phi\psi QV, X)\\
&+ g_M(h\nabla_U \phi V, CX)\\
&+ g_M(\mathcal{T}_{\mathcal{U}}\phi V, BX)\\
g_M(\nabla_U V, X) &= cos^2\theta_1\, g_M(\nabla_U PV, X)\\
&+ cos^2\theta_2\, g_M(\nabla_U QV, X)\\
&-g_M(h\nabla_U \phi\psi V, X)\\
&+g_M(\nabla_U \phi V, JX)
\end{aligned}$$

for $X \in \Gamma((ker\Phi_*)^{\perp})$ and $U, V \in \Gamma(ker\Phi_*)$. By using symmetry properties of second fundamental form of the map and conformality of the map, we obtain

$$\begin{aligned}
g_M(\nabla_U V, X) &= cos^2\theta_1\, g_M(\nabla_U PV, X)\\
&+ cos^2\theta_2\, g_M(\nabla_U QV, X)\\
&-\tfrac{1}{\lambda^2} g_N\left(\Phi_*\big(\mathcal{A}_{\phi\psi\mathcal{V}} U\big), \Phi_*(X)\right)\\
&+g_M(\nabla_U \phi V, JX)\\
g_M(\nabla_U V, X) &= cos^2\theta_1\, g_M(\nabla_U PV, X)\\
&+ cos^2\theta_2\, g_M(\nabla_U QV, X)\\
&-\lambda^{-2} g_N\big((\nabla\Phi_*)(\phi\psi V, U), \Phi_*(X)\big)\\
&+g_M(\nabla_U \phi V, JX).
\end{aligned}$$

From the last equation, we obtain the proof.

Theorem 3.11. Let Φ be a proper conformal bi-slant Riemannian map from a Kaehler manifold (M, g_M, J) to a Riemannian manifold (N, g_N) with slant angles θ_1 and θ_2. Then the total space M is a locally product manifold as $M_{D_1} \times M_{D_2} \times M_{(ker\Phi_*)^{\perp}}$ if and only if the equations in Theorem 3.6., Theorem 3.7. and Theorem 3.9. are hold where M_{D_1}, M_{D_2} and $M_{(ker\Phi_*)^{\perp}}$ are integral manifolds of the distributions D_1, D_2 and $(ker\Phi_*)^{\perp}$, respectively.

Theorem 3.12. Let Φ be a proper conformal bi-slant Riemannian map from a Kaehler manifold (M, g_M, J) to a Riemannian manifold (N, g_N) with slant angles θ_1 and θ_2. Then the total space M is a locally product manifold as $M_{(ker\Phi_*)^{\perp}} \times M_{ker\Phi_*}$ if and only if the equations in Theorem 3.9. and Theorem 3.10. are

hold where $M_{(ker\Phi_*)^\perp}$ and $M_{ker\Phi_*}$ are integral manifolds of the distributions $(ker\Phi_*)^\perp$ and $ker\Phi_*$, respectively.

Theorem 3.13. Let Φ be a proper conformal bi-slant Riemannian map from a Kaehler manifold (M, g_M, J) to a Riemannian manifold (N, g_N) with slant angles θ_1 and θ_2. Then, the map Φ is a totally geodesic map if and only if

$$\begin{aligned} g_N\left(\nabla^{\Phi}_{hE}\Phi_*(hG) - \nabla^{\Phi}_{E}\Phi_*(hG), \Phi_*(F)\right) &= \lambda^2 cos^2\,\theta_1\, g_M(\nabla_{vE}PvG, F) \\ &+ \lambda^2 cos^2\,\theta_2\, g_M(\nabla_{vE}QvG, F) \\ &+ \lambda^2 g_M(h\nabla_{vE}\phi\psi vG + \phi\mathcal{T}_{v\mathcal{E}}\phi vG \\ &+ Ch\nabla_{vE}\phi vG - \mathcal{A}_{\hbar\mathcal{E}}vG \\ &- h\nabla_{vE}hG, F) \\ &+ \lambda^2\{hE(ln\,\lambda)g_M(hG, F) \\ &+ hG(ln\,\lambda)g_M(hE, F) \\ &- F(ln\,\lambda)g_M(hE, hG)\} \end{aligned}$$

for $E, F, G \in \Gamma(TM)$.

Proof. Now, recall that Φ is said to be totally geodesic map if $(\nabla F_*)(E, G) = 0$ for all $E, G \in \Gamma(TM)$. By using this notion, we have

$$\begin{aligned} (\nabla\Phi_*)(E, G) &= \nabla^{\Phi}_{E}\Phi_*(hG) \\ &- \Phi_*(\nabla_{vE}vG + \mathcal{A}_{\hbar\mathcal{E}}vG + h\nabla_{vE}hG) \\ &+ (\nabla\Phi_*)(hE, hG) - \nabla^{\Phi}_{hE}\Phi_*(hG) \\ &= \nabla^{\Phi}_{E}\Phi_*(hG) \\ &-\Phi_*(\nabla_{vE}vG + \mathcal{A}_{\hbar\mathcal{E}}vG + h\nabla_{vE}hG) \\ &+(\nabla\Phi_*)^\perp(hE, hG) - \nabla^{\Phi}_{hE}\Phi_*(hG) \\ &+hE(ln\,\lambda)\Phi_*(hG) \\ &+hG(ln\,\lambda)\Phi_*(hE) \\ &-g_M(hE, hG)\Phi_*\big(grad(ln\,\lambda)\big). \end{aligned}$$

On the other hand, we get

$$\begin{aligned} -\Phi_*(\nabla_{vE}vG) &= cos^2\,\theta_1\,\Phi_*(\nabla_{vE}PvG) \\ &+ cos^2\,\theta_2\,\Phi_*(\nabla_{vE}QvG) \\ &+ \Phi_*(h\nabla_{vE}\phi\psi vG + \phi\mathcal{T}_{v\mathcal{E}}\phi vG \\ &+ Ch\nabla_{vE}\phi vG). \end{aligned}$$

Hence, by putting this equation into $(\nabla\Phi_*)(E, G)$, we obtain,

$$\begin{aligned} (\nabla\Phi_*)(E, G) &= \nabla^{\Phi}_{E}\Phi_*(hG) - \nabla^{\Phi}_{hE}\Phi_*(hG) \\ &+ cos^2\,\theta_1\,\Phi_*(\nabla_{vE}PvG) \\ &+ cos^2\,\theta_2\,\Phi_*(\nabla_{vE}QvG) \\ &+ \Phi_*(h\nabla_{vE}\phi\psi vG + \phi\mathcal{T}_{v\mathcal{E}}\phi vG \\ &+ Ch\nabla_{vE}\phi vG) - \Phi_*(\mathcal{A}_{\hbar\mathcal{E}}vG \\ &+ h\nabla_{vE}hG) + hE(ln\,\lambda)\Phi_*(hG) \\ &+hG(ln\,\lambda)\Phi_*(hE) \\ &-g_M(hE, hG)\Phi_*\big(grad(ln\,\lambda)\big). \end{aligned}$$

For $F \in \Gamma(TM)$, by applying $\Phi_*(F)$ to last equation and since the map is conformal Riemannian, we obtain

$$\begin{aligned} g_N\big((\nabla\Phi_*)(E, G), \Phi_*(F)\big) &= \\ g_N\left(\nabla^{\Phi}_{E}\Phi_*(hG) - \nabla^{\Phi}_{hE}\Phi_*(hG), \Phi_*(F)\right) & \\ +\lambda^2\,cos^2\,\theta_1\,g_M(\nabla_{vE}PvG, F) & \\ +\lambda^2\,cos^2\,\theta_2\,g_M(\nabla_{vE}QvG, F) & \\ +\lambda^2 g_M(h\nabla_{vE}\phi\psi vG + \phi\mathcal{T}_{v\mathcal{E}}\phi vG + Ch\nabla_{vE}\phi vG & \\ - \mathcal{A}_{\hbar\mathcal{E}}vG - h\nabla_{vE}hG, F) & \\ +\lambda^2\{hE(ln\,\lambda)g_M(hG, F) + hG(ln\,\lambda)g_M(hE, F) & \\ - F(ln\,\lambda)g_M(hE, hG)\}. & \end{aligned}$$

Therefore, the proof is clear.

4. Discussion

Since we have the definition of conformal Riemannian map and bi-slant structure properties, these notions are combined as conformal bi-slant Riemannian map. In this study, we examine its some geometric properties.

References

AKYOL, M.A., ŞAHİN, B. (2019). Conformal slant submersions. *Hacettepe Journal of Mathematics and Statistics*, 48(1), 28-44.

AYKURT SEPET, S. (2020). Pointwise bi-slant submersions. *Celal Bayar University Journal of Science*, 16(3), 339-343.

AYKURT SEPET, S. (2021). Conformal bi-slant submersions. *Turkish Journal of Mathematics*, 45, 1705-1723.

BAIRD, P., WOOD, J.C. (2003). Harmonic Morphisms between Riemannian manifolds, Oxford University Press.

FALCITELLI, M., IANUS S., PASTORE, A.M. (2004). Riemannian Submersions and Related Topics, World Scientific.

FISCHER, A.E. (1992). Riemannian maps between Riemannian manifolds. *Contemporary Mathematics*, 132, 331-366.

GRAY, A. (1967). Pseudo-Riemannian almost product manifolds and submersions. *Journal of Mathematics and Mechanics*, 16(7), 715-737.

NORE, T. (1986). Second fundamental form of a map. *Annali di Matematica Pura ed Applicata*, *146*, 281-310.

O'NEILL, B. (1966). The fundamental equations of a submersion. *Michigan Mathematical Journal*, 13, 458-469.

ŞAHİN, B. (2010). Conformal Riemannian maps between Riemannian manifolds, their harmonicity and decomposition theorems. *Acta Applicandae Mathematicae*, 109(3), 829-847.

ŞAHİN, B. (2017). Riemannian Submersions, Riemannian Maps in Hermitian Geometry, and Their Applications, Academic Press, Elsevier.

ŞAHİN, B., YANAN, Ş. (2018). Conformal Riemannian maps from almost Hermitian manifolds. *Turkish Journal of Mathematics*, 42(5), 2436-2451.

ŞAHİN, B., YANAN, Ş. (2019). Conformal semi-invariant Riemannian maps from almost Hermitian manifolds. *Filomat*, 33(4), 1125-1134.

WATSON, B. (1976). Almost Hermitian submersions. *Journal of Differential Geometry*, 11(1), 147-165.

YANAN, Ş. (2021). Conformal generic Riemannian maps from almost Hermitian manifolds. *Turkish Journal of Science*, 6(2), 76-88.

YANAN, Ş. (2022a). Conformal hemi-slant Riemannian maps. *Fundamentals of Contemporary Mathematical Sciences*, 3(1), 57-74.

YANAN, Ş. (2022b). Conformal semi-slant Riemannian maps from almost Hermitian manifolds onto Riemannian manifolds. *Filomat*, 36(5).

YANAN, Ş., ŞAHİN, B. (2022). Conformal slant Riemannian maps. *International Journal of Maps in Mathematics*, 5(1), 78-100.

YANO, K., KON, M. (1984). Structures on manifolds, World Scientific.

Evaluation of mRNA Expression Levels of IL-10, IL-12, TGF-β, FOXP3, IFN in Multiple Sclerosis Patients

Ayşe CEYLAN[1], Nuray BİLGE[2], Eda BALKAN[1*]

[1] *Department of Medical Biology, Faculty of Medicine, Atatürk University, Erzurum, Turkey*

aysealbayrak13@hotmail.com, edadiyarbakir@atauni.edu.tr

[2] *Department of Neurology, Faculty of Medicine, Atatürk University, Erzurum, Turkey*

nuray.bilge@atauni.edu.tr

Abstract

Although great advances have been made in the treatment of Multiple Sclerosis (MS), a neurodegenerative disease due to autoimmune inflammation, the etiopathogenesis of the disease has not yet been fully understood. Therefore, current treatment strategies may be insufficient. This study, it was aimed to quantitatively measure the expression levels of some cytokines determined in patients receiving MS treatment. This study was carried out on patients diagnosed with MS and healthy volunteers followed in Atatürk University Health Research and Application Center Neurology Department, Erzurum, Turkey. mRNA expression changes of *IL-10*, *IL-12*, *TGF-β, FOXP3,* and *IFN* genes in blood samples taken from both groups were determined by quantitative Real-Time PCR. It was determined that there was no statistically significant difference between the patient and control group in the mRNA expression levels of the *IL-10* and *FOXP3* genes. A statistically significant difference was observed between the patient and control group in *TGF-β, IL-12*, and *IFN* mRNA levels. In this study, it was determined that important information about the course of the disease can be obtained by evaluating the expression levels of regulator genes in MS, together.

Keywords: Biomarker, Cytokines, Gene expression, Multiple sclerosis.

Received:22.03.2022
Accepted:22.06.2022
Published:30.06.2022
[*]*Corresponding author:* Eda BALKAN, *PhD*
Department of Medical Biology, Faculty of Medicine, Atatürk University
E-mail: edadiyarbakir@atauni.edu.tr
Cite this article as: E. Balkan, Evaluation of mRNA Expression Levels of IL-10, IL-12, TGF-β, FOXP3, IFN in Multiple Sclerosis Patients, *Eastern Anatolian Journal of Science, Vol. 8, Issue 1, 9-14, 2022.*

1. Introduction

Multiple sclerosis (MS) is common and a chronic neurological disease characterized by damage to axons and myelin in the central nervous system, leading to various manifestations such as cognitive problems, motor control, depression, and fatigue (Ascherio et al., 2012; Dobson & Giovannoni, 2019). Although genetic predisposition contributes to MS pathology, environmental factors such as ultraviolet exposure, obesity, and smoking are also known to play a role in the onset and progression of the disease (Ascherio, 2013). However, the etiology of MS remains unclear, as it is a multifactorial, heterogeneous, and immune-mediated neurodegenerative disease (Filippi et al., 2018).

Genome-wide association (GWAS) studies have identified more than 200 risk variants, most of which are associated with genes that control immune cell function and contribute to genetic susceptibility to disease risk (Baranzini & Oksenberg, 2017). The results show that the disease is mostly due to the dysregulation of pro and anti-inflammatory cytokines. Pro-inflammatory cytokines cause an increase in the permeability of the blood-brain barrier (BBB), leading to neurodegeneration and demyelination of the central nervous system, while anti-inflammatory cytokines can suppress the secretion of pro-inflammatory cytokines (Hashemi et al., 2018). Therefore, it is emphasized that inflammation may play a crucial roles in axon and neuron degeneration,

which is prominent in MS pathology (Hashemi et al., 2020).

Autoreactive CD4+ T cells differentiate into pathogenic helper T (Th) cells (Th1 and Th17) in secondary lymphoid organs, causing the production of proinflammatory cytokines and increased subpial blood vessel permeability, resulting in the escape of circulating autoreactive T cells and effector myeloid cells. Cytokines produced by these subtype cells such as Th1 and Th17 are dynamic players of the inflammatory process, which is considered important for the development of MS (Arellano et al., 2017). Cytokines produced by infiltrating immune cells are implicated throughout the entire course of the disease, from T-cell differentiation to tissue inflammation and damage in the CNS (Palle et al., 2017). Thus, previous studies have proven that cytokine availability and/or signaling management can be an effective approach for the therapy of MS as in different autoimmune diseases (Mirshafiey & Mohsenzadegan, 2009; Williams et al., 2014).

Considering this complex and heterogeneous mechanism of MS, detecting the change in immune response may help identify validated biomarkers that can be used in disease diagnosis and diagnosis. Defining the alterations in the expression levels of critical genes involved in the disease is considered very valuable in terms of contributing to the determination of the effective treatment approach to be applied to individuals who have been treated for MS, as well as elucidating the critical molecular mechanisms for the disease (Hendrickx et al., 2017). This study, it was aimed to contribute to the elucidation of the etiology of the disease through relevant molecular factors by detecting the changes in the mRNA expression levels of some cytokines in patients diagnosed with MS and healthy control groups.

2. Materials and Methods

2.1. Sample collection and ethics statement

This study was carried out in a patient group consisting of 30 patients (18 females - 12 males, newly diagnosed with MS and not taking any medication) who were followed in Erzurum Atatürk University Health Research and Application Center Directorate Neurology Department Polyclinic and diagnosed with MS (according to 2010 McDonald Diagnostic Criteria) and 20 healthy (13 females - 7 males) without any systemic disease carried out on a control group of individuals. Those who were in the MS attack period and received cortisone treatment in the last three months were excluded from the study. The patient and control group who agreed to participate in the study signed the informed consent form, and the clinical and laboratory parameters of the patient group and the drugs used were recorded in the Neurology Patient Anamnesis Forms. This study was approved by the Atatürk University Faculty of Medicine Clinical Research Ethics Committee (05/01-07.06.2018). Detailed sampling informations are summarized in Table 1.

Table 1. Demographic and clinical characteristics of the samples. EDSS: Extended Disability Status Scale, RRMS: Relapsing remitting multipl skleroz

	MS (30)	**Control (20)**
Age (mean ± SD)	38.43 ± 7.62	35.37 ± 8.81
Sex (% female/male)	60/40	65/35
EDSS (mean ± SD)	1.72 ± 0.87	1.82 ± 1.24
MS Type	RRMS	-
Sampling Date(s)	01/09/2018-01/01/2019	

2.2. Gene expression analysis

Total RNA extraction from the blood samples collected from the patient and control groups was performed using a commercial isolation kit (NucleoSpin® RNA Blood, Macherey-Nagel, Germany). The procedure and chemicals recommended by the manufacturer were used for isolation. The concentration and purity of the obtained RNAs were determined using a NanoDrop spectrophotometer (MaestroNano - USA). The obtained products were stored at -80 °C until use. cDNA was synthesized using the ProtoScript® II First Strand cDNA Synthesis Kit (NEB, USA) according to the manufacturer's protocol. All cDNAs were stored at –20°C until use.

mRNA expression profiles of interleukin 10 (*IL-10*), interleukin 12 (*IL-12*), transforming growth factor-beta (*TGF-β*), interferon (*IFN*), and forkhead box P3 (*FOXP3*) genes were measured using the Taqman (GoTaq® Probe qPCR Master Mix, Promega) based qPCR method. qPCR reactions were

performed in a Roche LightCycler 480 (Roche Diagnostics). The amounts of the components that make up the reaction mixture in each tube and the amplification temperature conditions were determined following the protocol recommended by the manufacturer. All measurements were analyzed in triplicate for each sample. Beta-actin (ACTB) was used as a reference gene (housekeeping) for the normalization of target genes.

2.3. Statistical analysis

SPSS 20.0 (Statistical Packages for the Social Sciences for Windows XP Release 20.0 version) program was used to evaluate all statistical data related to the study. A Chi-square test was performed on the patient and control groups. Statistically significant differences are presented as follows: $p > 0.05$ (not significant, ns) and $p < 0.05$ (significant).

3. Results

In this study, the mRNA expression levels of IL-10, IL-12, TGF-β, IFN, and FOXP3 genes were investigated from peripheral blood samples collected from 30 patients with MS and 20 healthy individuals.

According to the findings; It was determined that there was a significant difference in the mRNA expression levels of *IL-12, IFN, TGF-β* genes in patients diagnosed with MS compared to the control group. There was no significant difference between the patient and control groups in *IL-10* and *FOXP3* expression levels. The averages and significance levels of the expression levels of the relevant genes are summarized in Figure 1 and Table 1.

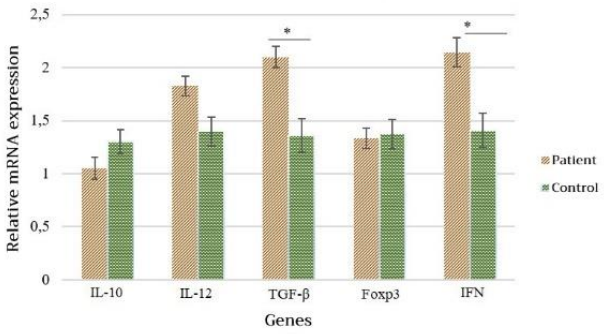

Figure 1. Comparison of expression levels of all genes (*: p<0.005)

Table 1. Patient and control group gene expression levels. MS: Multiple sclerosis, n: total number of subjects sampled

Gene symbol	MS (30) median	Control (20) median	*p* value
IL-10	7.41	10.183	>0.05
IL-12	15.54	10.056	<0.05
TGF-β	13.9	9.736	<0.005
FOXP3	10.02	10.179	>0.05
IFN	18.05	12.087	<0.005

4. Discussion

The incidence of MS, a common non-traumatic disease that mostly affects young adults, is increasing worldwide, due to the socioeconomic impact of the disease (Balkan & Bilge, 2021; Kobelt et al., 2017). Although the mechanisms underlying the disease are not fully understood, gene-environment interactions are thought to play an prominent role (Browne et al., 2014). Today, advances in the diagnostic methods and criteria used for MS, together with the developing technology, enable the diagnosis of the disease to be made at earlier stages. For this reason, the hypothesis that key genes identified in the light of available information and determined to be associated with the disease can be used as biomarkers gains more importance (Monforte & McPhail, 2005). Identification of confirmed biomarkers based on gene expression approach increases the chance of early diagnosis/diagnosis for the related disease, as well as in terms of determining an effective treatment approach (van't Veer et al., 2005; Wei et al., 2004). Therefore, in this study, the most important members of many different major gene groups known to be associated with MS (I*L-10, IL-12, TGF-β, IFN,* and *FOXP3*) were selected and their mRNA expression levels were evaluated together.

It is known that IL-12 production is very important systemically, as it can negatively affect the Th1 response and increase susceptibility to intercellular pathogens (Trinchieri, 1995). It has been determined by previous studies that the amount of IFN also increases by means of T cells that can be activated depending on the increased IL-12 (Balashov et al., 1997). Accordingly, in a study by Reiche et al., IL-12 and serum IFN levels were found to be higher in RR-MS (Relapsing-remitting MS) patients compared to controls (Kallaur et al., 2013). Different

studies have also shown that IL-12 and IFN levels are increased in the brain, cerebrospinal fluid (CSF), and peripheral blood of the patients (Huang et al., 2004). The results obtained in the present study are also in line with previous research.

TGF-β is a pleiotropic cytokine involved in the differentiation and function of T cells. Therefore, it is considered that it may have important functions in an immune system-related disease such as MS (Lee et al., 2017). Its immunosuppressive nature supports the hypothesis that a therapeutic approach to suppressing autoimmunity of TGF-β may be effective. In this direction, studies with rodent models suggest that the administration of TGF-β1 and TGF-β2 during the induction and progression stages of the disease shows positive results in terms of MS. It has been stated that relapse formation is prevented in mice injected with TGF-β1 and that TGF-β1 can be used as an anti-inflammatory due to its immunosuppressive feature against proinflammatory cytokines such as IL-1 (Kuruvilla et al., 1991). In addition, many studies have shown that fewer CNS lesions occur by reducing neurological damage with TGF-β administration (Johns et al., 1991). In the current study, results were obtained in parallel with previous studies, and it was observed that the expression level of *TGF-β* in MS patients increased significantly compared to the control as a result of drug treatment.

Finally, mRNA expression levels of the *FOXP3* gene were investigated in our study. FOXP3 is a transcription factor involved in the production and normal functioning of T cells (Isik et al., 2014). recent studies have confirmed the involvement of FOXP3 in the regulation of CD4+, CD25+, and Treg cells (Li et al., 2015). In the study performed by Taheri et al., it was observed that single nucleotide polymorphisms (SNPs) in the promoter seciton of the gene in question can change the expression level of the gene and the disease susceptibility may increase, consequently (Eftekharian et al., 2016). Studies conducted by different groups also reveal that the insufficiency of FOXP3 and similar mechanisms that prevent the development of pathogenic T cells may be a significant factor in the formation of autoimmune diseases such as MS (Huan et al., 2005). The results of our study also show that *FOXP3* mRNA expression is decreased in the MS group compared to the control group.

5. Conclusion

Although the etiology of MS is unknown, previous studies strengthen the hypothesis that it is a T cell-mediated autoimmune disease. Major genes related to MS were evaluated together in the current study to help understand the pathogenesis of MS and improve the life quality of patients by mediating the development of new and more effective methods in the treatment of the disease. It is thought that the findings obtained have the potential to shed light and form a basis for studies to be carried out to elucidate the molecular etiology of MS. However, there are several limitations to this study that should also be noted. The first of these is the small sample size. Therefore, further works should consider sampling size. Secondly, the genes targeted in this study need to be further examined at the protein level to verify the analysis results.

6. Acknowledgement

This study was supported by Atatürk University Scientific Research Projects Coordination Unit (Project Number: TYL-2019-7045).

Conflict of Interests

The authors declare that there is no potential conflict of interest for the research, authorship, and/or publication of this article. All authors read and approved the final manuscript.

Author Contributions

Design of the study: EB, Sample collection: NB, Performed the experiments: AC, Data Collection and/or Processing: EB, NB, AC, Writing Original Manuscript: EB, NB, AC. EB contributed to revising the work and final approval of the final version of the manuscript.

Ethical Approval

This study was approved by the Atatürk University Faculty of Medicine Clinical Research Ethics Committee (05/01-07.06.2018).

References

ARELLANO, G., ACUNA, E., REYES, L. I., OTTUM, P. A., DE SARNO, P., VILLARROEL, L., CIAMPI, E., URIBE-SAN MARTIN, R., CARCAMO, C., and NAVES, R. (2017). Th1 and Th17 Cells and Associated Cytokines Discriminate among Clinically Isolated Syndrome and Multiple Sclerosis Phenotypes. Front Immunol, 8, 753. doi:10.3389/fimmu.2017.00753

ASCHERIO, A. (2013). Environmental factors in multiple sclerosis. Expert Rev Neurother, 13(12 Suppl), 3-9. doi:10.1586/14737175.2013.865866

ASCHERIO, A., MUNGER, K. L., and LUNEMANN, J. D. (2012). The initiation and prevention of multiple sclerosis. Nat Rev Neurol, 8(11), 602-612. doi:10.1038/nrneurol.2012.198

BALASHOV, K. E., SMITH, D. R., KHOURY, S. J., HAFLER, D. A., and WEINER, H. L. (1997). Increased interleukin 12 production in progressive multiple sclerosis: induction by activated CD4+ T cells via CD40 ligand. Proc Natl Acad Sci U S A, 94(2), 599-603. doi:10.1073/pnas.94.2.599

BALKAN, E., and BILGE, N. (2021). Expression levels of IL-17/IL-23 cytokine-targeting microRNAs 20, 21, 26, 155, and Let-7 in patients with relapsing-remitting multiple sclerosis. Neurol Res, 43(9), 778-783. doi:10.1080/01616412.2021.1935099

BARANZINI, S. E., and OKSENBERG, J. R. (2017). The Genetics of Multiple Sclerosis: From 0 to 200 in 50 Years. Trends Genet, 33(12), 960-970. doi:10.1016/j.tig.2017.09.004

BROWNE, P., CHANDRARATNA, D., ANGOOD, C., TREMLETT, H., BAKER, C., TAYLOR, B. V., and THOMPSON, A. J. (2014). Atlas of Multiple Sclerosis 2013: A growing global problem with widespread inequity. Neurology, 83(11), 1022-1024. doi:10.1212/WNL.0000000000000768

DOBSON, R., and GIOVANNONI, G. (2019). Multiple sclerosis - a review. Eur J Neurol, 26(1), 27-40. doi:10.1111/ene.13819

EFTEKHARIAN, M. M., SAYAD, A., OMRANI, M. D., GHANNAD, M. S., NOROOZI, R., MAZDEH, M., MIRFAKHRAIE, R., MOVAFAGH, A., ROSHANAEI, G., AZIMI, T., INOKO, H., and TAHERI, M. (2016). Single nucleotide polymorphisms in the FOXP3 gene are associated with increased risk of relapsing-remitting multiple sclerosis. Hum Antibodies, 24(3-4), 85-90. doi:10.3233/HAB-160299

FILIPPI, M., BAR-OR, A., PIEHL, F., PREZIOSA, P., SOLARI, A., VUKUSIC, S., and ROCCA, M. A. (2018). Multiple sclerosis. Nat Rev Dis Primers, 4(1), 43. doi:10.1038/s41572-018-0041-4

HASHEMI, R., HOSSEINI-ASL, S. S., AREFHOSSEINI, S. R., and MORSHEDI, M. (2020). The impact of vitamin D3 intake on inflammatory markers in multiple sclerosis patients and their first-degree relatives. PLoS One, 15(4), e0231145. doi:10.1371/journal.pone.0231145

HASHEMI, R., MORSHEDI, M., ASGHARI JAFARABADI, M., ALTAFI, D., SAEED HOSSEINI-ASL, S., and RAFIE-AREFHOSSEINI, S. (2018). Anti-inflammatory effects of dietary vitamin D3 in patients with multiple sclerosis. Neurol Genet, 4(6), e278. doi:10.1212/NXG.0000000000000278

HENDRICKX, D. A. E., VAN SCHEPPINGEN, J., VAN DER POEL, M., BOSSERS, K., SCHUURMAN, K. G., VAN EDEN, C. G., HOL, E. M., HAMANN, J., and HUITINGA, I. (2017). Gene Expression Profiling of Multiple Sclerosis Pathology Identifies Early Patterns of Demyelination Surrounding Chronic Active Lesions. Front Immunol, 8, 1810. doi:10.3389/fimmu.2017.01810

HUAN, J., CULBERTSON, N., SPENCER, L., BARTHOLOMEW, R., BURROWS, G. G., CHOU, Y. K., BOURDETTE, D., ZIEGLER, S. F., OFFNER, H., and VANDENBARK, A. A. (2005). Decreased FOXP3 levels in multiple sclerosis patients. J Neurosci Res, 81(1), 45-52. doi:10.1002/jnr.20522

HUANG, W. X., HUANG, P., and HILLERT, J. (2004). Increased expression of caspase-1 and interleukin-18 in peripheral blood mononuclear cells in patients with multiple sclerosis. Mult Scler, 10(5), 482-487. doi:10.1191/1352458504ms1071oa

ISIK, N., YILDIZ MANUKYAN, N., AYDIN CANTURK, I., CANDAN, F., UNSAL CAKMAK, A., and SARU HAN DIRESKENELI, G. (2014). Genetic Susceptibility to Multiple Sclerosis: The Role of FOXP3 Gene Polymorphism. Noro Psikiyatr Ars, 51(1), 69-73. doi:10.4274/npa.y7098

JOHNS, L. D., FLANDERS, K. C., RANGES, G. E., and SRIRAM, S. (1991). Successful treatment of experimental allergic encephalomyelitis with transforming growth factor-beta 1. J

Immunol, 147(6), 1792-1796. Retrieved from https://www.ncbi.nlm.nih.gov/pubmed/17162779

KALLAUR, A. P., OLIVEIRA, S. R., COLADO SIMAO, A. N., DELICATO DE ALMEIDA, E. R., KAMINAMI MORIMOTO, H., LOPES, J., DE CARVALHO JENNINGS PEREIRA, W. L., MARQUES ANDRADE, R., MULITERNO PELEGRINO, L., DONIZETE BORELLI, S., KAIMEN-MACIEL, D. R., and REICHE, E. M. (2013). Cytokine profile in relapsingremitting multiple sclerosis patients and the association between progression and activity of the disease. Mol Med Rep, 7(3), 1010-1020. doi:10.3892/mmr.2013.1256

KOBELT, G., THOMPSON, A., BERG, J., GANNEDAHL, M., ERIKSSON, J., GROUP, M. S., and EUROPEAN MULTIPLE SCLEROSIS, P. (2017). New insights into the burden and costs of multiple sclerosis in Europe. Mult Scler, 23(8), 1123-1136. doi:10.1177/1352458517694432

KURUVILLA, A. P., SHAH, R., HOCHWALD, G. M., LIGGITT, H. D., PALLADINO, M. A., and THORBECKE, G. J. (1991). Protective effect of transforming growth factor beta 1 on experimental autoimmune diseases in mice. Proc Natl Acad Sci U S A, 88(7), 2918-2921. doi:10.1073/pnas.88.7.2918

LEE, P. W., SEVERIN, M. E., and LOVETT-RACKE, A. E. (2017). TGF-beta regulation of encephalitogenic and regulatory T cells in multiple sclerosis. Eur J Immunol, 47(3), 446-453. doi:10.1002/eji.201646716

LI, Z., LI, D., TSUN, A., and LI, B. (2015). FOXP3+ regulatory T cells and their functional regulation. Cell Mol Immunol, 12(5), 558-565. doi:10.1038/cmi.2015.10

MIRSHAFIEY, A., and MOHSENZADEGAN, M. (2009). TGF-beta as a promising option in the treatment of multiple sclerosis. Neuropharmacology, 56(6-7), 929-936. doi:10.1016/j.neuropharm.2009.02.007

MONFORTE, J., and MCPHAIL, S. (2005). Strategy for gene expression-based biomarker discovery. Biotechniques, Suppl, 25-29. doi:10.2144/05384su05

PALLE, P., MONAGHAN, K. L., MILNE, S. M., and WAN, E. C. K. (2017). Cytokine Signaling in Multiple Sclerosis and Its Therapeutic Applications. Med Sci (Basel), 5(4). doi:10.3390/medsci5040023

TRINCHIERI, G. (1995). Interleukin-12: a proinflammatory cytokine with immunoregulatory functions that bridge innate resistance and antigen-specific adaptive immunity. Annu Rev Immunol, 13, 251-276. doi:10.1146/annurev.iy.13.040195.001343

VAN'T VEER, L. J., PAIK, S., and HAYES, D. F. (2005). Gene expression profiling of breast cancer: a new tumor marker. J Clin Oncol, 23(8), 1631-1635. doi:10.1200/JCO.2005.12.005

WEI, J. S., GREER, B. T., WESTERMANN, F., STEINBERG, S. M., SON, C. G., CHEN, Q. R., WHITEFORD, C. C., BILKE, S., KRASNOSELSKY, A. L., CENACCHI, N., CATCHPOOLE, D., BERTHOLD, F., SCHWAB, M., and KHAN, J. (2004). Prediction of clinical outcome using gene expression profiling and artificial neural networks for patients with neuroblastoma. Cancer Res, 64(19), 6883-6891. doi:10.1158/0008-5472.CAN-04-0695

WILLIAMS, S. K., MAIER, O., FISCHER, R., FAIRLESS, R., HOCHMEISTER, S., STOJIC, A., PICK, L., HAAR, D., MUSIOL, S., STORCH, M. K., PFIZENMAIER, K., and DIEM, R. (2014). Antibody-mediated inhibition of TNFR1 attenuates disease in a mouse model of multiple sclerosis. PLoS One, 9(2), e90117. doi:10.1371/journal.pone.0090117

On Hyperbolic Padovan and Hyperbolic Pell-Padovan Sequences

Sait TAŞ[1]

[1] *Department of Mathematics, University of Atatürk, Erzurum, Turkey*
saittas@atauni.edu.tr,

Abstract

In this article, we extend Padovan and Pell-Padovan numbers to Hyperbolic Padovan and Hyperbolic Pell-Padovan numbers, respectively. Moreover, we obtain Binet-like formulas, generating functions and some identities related to Hyperbolic Padovan and Hyperbolic Pell-Padovan numbers.

Keywords: Padovan numbers, Pell-Padovan numbers, Hyperbolic numbers, Hyperbolic Padovan numbers, Hyperbolic Pell-Padovan numbers..

1. Introduction

Hyperbolic numbers have applications in different areas of mathematics and theoretical physics. In particular, they are related to Lorentz-Minkowski (Space-time) geometry in the plane as well as complex numbers (Catoni 2008). The work on the function theory for hyperbolic numbers can be found in (Aydın 2019, Barreira 2016, Berzsenyi 1977, Deveci 2020, Güncan 2012, Horadam 1963, Khadjiev 2016, Motter 2016, Taş 2021, Taşçı 2018). The set of hyperbolic numbers H can be described in the form

$$\mathbb{H} = \{z = x + hy \mid h \notin \mathbb{R}, h^2 = 1, x, y \in \mathbb{R}\}$$

Addition, subtraction and multiplication of two hyperbolic numbers z_1 and z_2 are defined by

$$z_1 \pm z_2 = (x_1 + hy_1) \pm (x_2 + hy_2) = (x_1 \pm x_2) + h(y_1 \pm y_2)$$

$$z_1 \times z_2 = (x_1 + hy_1) \times (x_2 + hy_2) = (x_1x_2) + (y_1y_2) + h(x_1y_2 + y_1x_2)$$

On the other hand, the division of two hyperbolic numbers is given by

$$\frac{z_1}{z_2} = \frac{x_1 + hy_1}{x_2 + hy_2}$$

$$\frac{(x_1 + hy_1)(x_2 - hy_2)}{(x_2 + hy_2)(x_2 - hy_2)} = \frac{x_1x_2 + y_1y_2}{x_2^2 - y_2^2} + h\frac{(x_1y_2 + y_1x_2)}{x_2^2 - y_2^2}$$

If $x_2^2 - y_2^2 \neq 0$, then the division $\frac{z_1}{z_2}$ is possible. The hyperbolic conjugation of $z = x + hy$ is defined by $\bar{z} = x - hy$.

2. Materials and Methods

Padovan sequence is named after Richard Padovan (Voet 2012) and (Çağman 2021a, Çağman 2021b, Deveci 2015, Deveci 2018, Shannon 2006, Taş 2014) studied Padovan sequence and Pell- Padovan sequence.

The Padovan sequence is the sequence of integers P_n defined by the initial values $P_0 = P_1 = P_2 = 1$ and the recurrence relation

$$P_n = P_{n-2} + P_{n-3}$$

for all $n \geq 3$. The first few values of P_n are $1, 1, 1, 2, 2, 3, 4, 5, 7, 9, 12, 16, 21, 28, 37$.

Pell-Padovan sequence is defined by the initial values $R_0 = R_1 = R_2 = 1$ and the recurrence relation

$$R_n = 2R_{n-2} + R_{n-3}$$

for all $n \geq 3$. The first few values of R_n are $1, 1, 1, 3, 3, 3, 7, 9, 17, 25, 43, 67, 111, 177, 289$.

Received:05.04.2022
Accepted:11.05.2022
Published:30.06.2022
**Corresponding author:* Sait TAŞ, *PhD*
Atatürk University, Faculty of Science, Department of Mathematics, Erzurum, Turkey
E-mail: saittas@atauni.edu.tr
Cite this article as: S.Taş, On Hyperbolic Padovan and Hyperbolic Pell-Padovan Sequences, *Eastern Anatolian Journal of Science, Vol. 8, Issue 1, 15-19, 2022.*

3. Results

Firstly, we give the definition of Hyperbolic Padovan sequence.

Definition 3.1. The Hyperbolic Padovan sequence is the sequence of hyperbolic numbers HP_n defined by the initial values $HP_0 = 1 + h, HP_1 = 1 + h, HP_2 = 1 + 2h$ and the recurrence relation

$$HP_n = P_n + hP_{n+1}$$
$$HP_n = HP_{n-2} + HP_{n-3}$$

for all $n \geq 3$.

The first few values of HP_n are $1 + h, 1 + h, 1 + 2h, 2 + 2h, 2 + 3h, 3 + 4h, 4 + 5h, 5 + 7h, 7 + 9h, 9 + 12h, 12 + 16h, 16 + 21h, 21 + 28h, 28 + 37h$.

Theorem 3.1. The generating function of the Hyperbolic Padovan sequence is

$$g(x) = \frac{1 + h + (1 + h)x + hx^2}{1 - x^2 - x^3}$$

Proof. Let

$$g(x) = \sum_{n=0}^{\infty} HP_n x^n = HP_0 + HP_1 x + HP_2 x^2 + HP_3 x^3 + \cdots + HP_n x^n + \cdots$$

be generating function of the Hyperbolic Padovan sequence. On the other hand, since

$$x^2 g(x) = HP_0 x^2 + HP_1 x^3 + HP_2 x^4 + HP_3 x^5 + \cdots + HP_{n-2} x^n + \cdots$$

and

$$x^3 g(x) = HP_0 x^3 + HP_1 x^4 + HP_2 x^5 + HP_3 x^6 + \cdots + HP_{n-3} x^n + \cdots$$

we write

$$(1 - x^2 - x^3)g(x) = HP_0 + HP_1 x + (HP_2 - HP_0)x^2 + (HP_3 - HP_1 - HP_0)x^3 + \cdots + (HP_n - HP_{n-2} - HP_{n-3})x^n + \cdots$$

Now consider $HP_0 = 1 + h, HP_1 = 1 + h, HP_2 = 1 + 2h$ and $HP_n = HP_{n-2} + HP_{n-3}$. Thus, we obtain

$$(1 - x^2 - x^3)g(x) = HP_0 + HP_1 x + (HP_2 - HP_0)x^2$$

$$(1 - x^2 - x^3)g(x) = 1 + h + (1 + h)x + hx^2$$

or

$$g(x) = \frac{1 + h + (1 + h)x + hx^2}{1 - x^2 - x^3}$$

Hence the proof is completed.

Now we give Binet-like formula for the Hyperbolic Padovan sequence.

Theorem 3.2. Binet-like formula for the Hyperbolic Padovan sequence is

$$HP_n = \left(a + h\frac{a}{r_1}\right)r_1^n + \left(b + h\frac{b}{r_2}\right)r_2^n + \left(c + h\frac{c}{r_3}\right)r_3^n$$

where

$$a = \frac{(r_2 - 1)(r_3 - 1)}{(r_1 - r_2)(r_1 - r_3)}, b = \frac{(r_1 - 1)(r_3 - 1)}{(r_2 - r_1)(r_2 - r_3)}, c = \frac{(r_1 - 1)(r_2 - 1)}{(r_1 - r_3)(r_2 - r_3)}$$

and r_1, r_2, r_3 are the roots of the equation $x^3 - x^2 - 1 = 0$.

Proof. It is easily seen that

$$HP_n = P_n + hP_{n+1}$$

On the other hand, we know that the Binet-like formula for the Padovan sequence is

$$P_n = \frac{(r_2 - 1)(r_3 - 1)}{(r_1 - r_2)(r_1 - r_3)}r_1^n + \frac{(r_1 - 1)(r_3 - 1)}{(r_2 - r_1)(r_2 - r_3)}r_2^n + \frac{(r_1 - 1)(r_2 - 1)}{(r_1 - r_3)(r_2 - r_3)}r_3^n.$$

Theorem 3.3.

$$\sum_{k=0}^{n} HP_k = HP_n + HP_{n+1} + HP_{n+2} - (2 + 3h).$$

Proof. By the definition of Hyperbolic Padovan sequence recurrence relation

$$HP_n = HP_{n-2} + HP_{n-3}$$

and

$$HP_0 = HP_2 - HP_{-1}$$
$$HP_1 = HP_3 - HP_0$$
$$HP_2 = HP_4 + HP_1$$
$$\vdots$$
$$HP_{n-2} = HP_n - HP_{n-3}$$
$$HP_{n-1} = HP_{n+1} - HP_{n-2}$$
$$HP_n = HP_{n+2} - HP_{n-1}$$

Then we have

$$\sum_{k=0}^{n} HP_k = HP_n + HP_{n+1} + HP_{n+2} - HP_{-1} - HP_0 - HP_1.$$

Now considering $HP_{-1} = h, HP_0 = 1 + h, HP_1 = 1 + h$ we write

$$\sum_{k=0}^{n} HP_k = HP_n + HP_{n+1} + HP_{n+2} - (2 + 3h)$$

and hence the proof is completed.

Now we investigate the new property of Hyperbolic Padovan numbers in relation to the Padovan matrix formula. We consider the following matrices:

$$Q_3 = \begin{bmatrix} 0 & 1 & 1 \\ 1 & 0 & 0 \\ 0 & 1 & 0 \end{bmatrix}, K_3 = \begin{bmatrix} 1+2h & 1+h & 1+h \\ 1+h & 1+h & h \\ 1+h & h & 1 \end{bmatrix}$$

and

$$M_3^n = \begin{bmatrix} HP_{n+2} & HP_{n+1} & HP_n \\ HP_{n+1} & HP_n & HP_{n-1} \\ HP_n & HP_{n-1} & HP_{n-2} \end{bmatrix}$$

Theorem 3.4. For all $n \in \mathbb{Z}^+$ we have

$$Q_3^n K_3 = M_3^n.$$

Proof. The proof is easily seen that using the induction on n.

As well-known Pell-Padovan sequence is defined by the recurrence relation

$$R_n = 2R_{n-2} + R_{n-3}$$

and the initial values $R_0 = R_1 = R_2 = 1$.

Now we define Hyperbolic Pell-Padovan sequence.

Definition 3.2. The Hyperbolic Pell-Padovan sequence is defined by the recurrence relation

$$HR_n = R_n + hR_{n-1}$$

$$HR_n = 2HR_{n-2} + HR_{n-3}$$

and the initial values $HR_0 = 1 - h, HR_1 = 1 + h, HR_2 = 1 + h$.

The first few values of HR_n are $1 - h, 1 + h, 1 + h, 3 + h, 3 + 3h, 7 + 3h, 9 + 7h$.

Theorem 3.5. Be the generating function of Hyperbolic Pell-Padovan sequence is

$$g(x) = \frac{1 - h + (1 + h)x + (-1 + 3h)x^2}{1 - 2x^2 - x^3}$$

Proof. Let

$$g(x) = \sum_{n=0}^{\infty} HR_n x^n = Hr_0 + HR_1 x + HR_2 x^2 + HR_3 x^3 + \cdots + HR_n x^n + \cdots$$

be the generating function of the Hyperbolic Pell-Padovan sequence. On the other hand, since

$$2x^2 g(x) = 2HR_0 x^2 + 2HR_1 x^3 + 2HR_2 x^4 + 2HR_3 x^5 + \cdots + 2HR_{n-2} x^n + \cdots$$

and

$$x^3 g(x) = HR_0 x^3 + HR_1 x^4 + HR_2 x^5 + HR_3 x^6 + \cdots + HR_{n-3} x^n + \cdots$$

we write

$$(1 - 2x^2 - x^3)g(x) = HR_0 + HR_1 x + (HR_2 - 2HP_0)x^2 + (HR_3 - 2HR_1 - HR_0)x^3 + \cdots + (HR_n - 2HR_{n-2} - HR_{n-3})x^n + \cdots$$

Now consider $HR_0 = 1 - h, HR_1 = 1 + h, HR_2 = 1 + h$ and $HR_n = 2HR_{n-2} + HR_{n-3}$. Thus, we obtain

$$(1 - 2x^2 - x^3)g(x) = HR_0 + HR_1 x + (HR_2 - 2HR_0)x^2$$

$$(1 - 2x^2 - x^3)g(x) = 1 - h + (1 + h)x + (-1 + 3h)x^2$$

or

$$g(x) = \frac{1 - h + (1 + h)x + (-1 + 3h)x^2}{1 - 2x^2 - x^3}$$

Hence the proof is completed.

Theorem 3.6. The Binet-like formula of Hyperbolic Pell-Padovan sequence is

$$HR_n = \frac{2(\alpha + h)}{\alpha - \beta}\left(1 - \frac{1}{\alpha}\right)\alpha^n - \frac{2(\beta + h)}{\alpha - \beta}\left(1 - \frac{1}{\beta}\right)\beta^n + (1 - h)\gamma^n$$

where

$$\alpha = \frac{1 + \sqrt{5}}{2}, \beta = \frac{1 - \sqrt{5}}{2}, \gamma = -1$$

are roots of the equation $x^3 - 2x - 1 = 0$.

Proof. The Binet-like formula of Pell-Padovan sequence is given

$$R_n = 2\frac{\alpha^{n+1}-\beta^{n+1}}{\alpha-\beta} - 2\frac{\alpha^n-\beta^n}{\alpha-\beta} + \gamma^{n+1}.$$

Now consider

$$HR_n = R_n + hR_{n-1}$$

so the proof is easily.

Theorem 3.7.

$$\sum_{k=0}^{n} HR_k = \frac{1}{2}[(-1-3h) - HR_{n+1} + HR_{n+2} + HR_{n+3}].$$

Proof. We know that

$$\sum_{k=0}^{n} R_k = \frac{1}{2}[-1 - R_{n+1} + R_{n+2} + R_{n+3}]$$

and

$$\sum_{k=0}^{n} R_{k-1} = \frac{1}{2}[-3 - 2R_n - R_{n+1} + R_{n+2} + R_{n+3}].$$

Since

$$HR_n = R_n + hR_{n-1}$$

we have

$$\sum_{k=0}^{n} HR_k = \sum_{k=0}^{n} R_k + h\sum_{k=0}^{n} R_{k-1}.$$

So the theorem is proved.

Theorem 3.8.

$$\sum_{k=1}^{n} HR_{2k} = R_{2n+1} + hR_{2n} - (n+1) + h(n-1).$$

Proof. If we consider the following equalities, then the proof is seen

$$\sum_{k=1}^{n} R_{2k} = R_{2n+1} - (n+1)$$

and

$$\sum_{k=1}^{n} R_{2k-1} = R_{2n} + (n-1).$$

Since

$$HR_n = R_n + hR_{n-1}$$

we have

$$\sum_{k=1}^{n} HR_{2k} = \sum_{k=1}^{n} R_{2k} + h\sum_{k=1}^{n} R_{2k-1}.$$

So the theorem is proved.

Now we investigate the new property of Hyperbolic Pell-Padovan numbers in relation to the Pell-Padovan matrix formula. We consider the following matrices:

$$Q_3 = \begin{bmatrix} 0 & 2 & 1 \\ 1 & 0 & 0 \\ 0 & 1 & 0 \end{bmatrix},$$

$$K_3 = \begin{bmatrix} 1+h & 1+h & 1-h \\ 1+h & 1-h & -1+3h \\ 1-h & -1+3h & 3-5h \end{bmatrix}$$

and

$$M_3^n = \begin{bmatrix} HR_{n+2} & HR_{n+1} & HR_n \\ HR_{n+1} & HR_n & HR_{n-1} \\ HR_n & HR_{n-1} & HR_{n-2} \end{bmatrix}$$

Theorem 3.9. For all $n \in \mathbb{Z}^+$ we have

$$Q_3^n K_3 = M_3^n.$$

Proof. The proof can be obtained easily by induction on n.

Theorem 3.10. If

$$P = \begin{bmatrix} 0 & 1 & 0 \\ 0 & 0 & 1 \\ 1 & 2 & 0 \end{bmatrix}$$

then we have

$$\begin{bmatrix} 0 & 1 & 0 \\ 0 & 0 & 1 \\ 1 & 2 & 0 \end{bmatrix}^n \begin{bmatrix} 1-h \\ 1+h \\ 1+h \end{bmatrix} = \begin{bmatrix} HR_n \\ HR_{n+1} \\ HR_{n+2} \end{bmatrix}.$$

Proof. The proof can be seen by mathematical induction on n.

4. Discussion

We defined Hyperbolic Padovan and Hyperbolic Pell-Padovan numbers and we obtain Binet-like formulas, generating functions and some identities related to Hyperbolic Padovan and Hyperbolic Pell-Padovan numbers.

References

ATANASSOV, K., DIMITROV, D., SHANNON, A., (2009). A remark on ψ-function and pell-padovan's sequence. *Notes on Number Theory and Discrete Mathematics, 15(2), 1-44.*

AYDIN, F.T., (2019). Hyperbolic Fibonacci sequence, *Universal Journal of Mathematics and Applications, 2(2), 59-64.*

BARREİRA, L., POPESCU, L.H., VALLS, C., (2016). Hyperbolic sequences of linear operators and evolution maps, *Milan Journal of Mathematics*, 84(2), 203-216.

BERZSENYİ, G., (1977). Gaussian fibonacci numbers.

CATONİ, F., BOCCALETTİ, D., CANNATA, R., CATONİ, V., NİCHELATTİ, E., ZAMPETTİ, P., (2008). The mathematics of Minkowski space-time: with an introduction to commutative hypercomplex numbers, *Springer Science & Business Media*,

ÇAĞMAN, A., (2021). Repdigits as Product of Fibonacci and Pell numbers, *Turkish Journal of Science , 6 (1) , 31-35* .

ÇAĞMAN, A., (2021). An approach to Pillai's problem with the Pell sequence and the powers of 3, *Miskolc Mathematical Notes 22 (2), 599-610*.

DEVECİ, Ö., KARADUMAN, E., (2015). The pell sequences in finite groups, *Util. Math, 96, 263-276*.

DEVECİ, Ö., SAHANNON, A.G., (2018). The quaternion-pell sequence, *Communications in Algebra, 46(12), 5403-5409.*

DEVECİ, Ö., SAHANNON, A.G., (2020). The complex-type k-fibonacci sequences and their applications, *Communications in Algebra, 46(12), pages 1-16.*

GARGOUBİ, H., KOSSENTİNİ, S., (2016). f-algebra structure on hyperbolic numbers. *Advances in Applied Clifford Algebras, 26(4), 1211-1233.*

GÜNCAN, A., ERBİL, Y., (2012). The q-fibonacci hyperbolic functions, *In AIP Conference Proceedings, American Institute of Physics, volume 1479, pages 946-949.*

HORADAM, A.F., (1963). Complex fibonacci numbers and fibonacci quaternions, *The American Mathematical Monthly, 70(3), 289-291*.

KHADJİEV, D., GÖKSAL, Y. (2016). Applications of hyperbolic numbers to the invariant theory in two-dimensional pseudo-euclidean space. *Advances in Applied Clifford Algebras, 26(2), 645-668.*.

MOTTER, A.E., ROSA, M.A.F. (2016). Hyperbolic calculus. *Advances in Applied Clifford Algebras, 8(1), 109-128.*

SHANNON, A.G., ANDERSON, P.G., HORADAM, A.F. (2006). Properties of cordonnier, perrin and van der laan numbers, *International Journal of Mathematical Education in Science and Technology, 37(7), 825-831.*

TAŞ, S. (2021). The Hyperpolic Quadrapell Sequences. *Eastern Anatolian Journal of Science, Volume VII, Issue I, 25-29.*

TAŞ, S., DEVECİ, Ö., KARADUMAN, E. (2014). The fibonacci-padovan sequences in fnite groups. *Maejo International Journal of Science And Technology, 2014, 8(3), 279-287.*

TAŞÇI, D. (2018). Gaussian padovan and gaussian pell-padovan sequences, *Communications Faculty of Sciences University of Ankara Series A1 Mathematics and Statistics*, 67(2), 82-88.

VOET, C. (2012). The poetics of order: Dom hans van der laan's architectonic space", *Architectural Research Quarterly*, 16(2), 137.

Forecasting Call Center Arrivals Using XGBoost Combined with Consecutive and Periodic Lookback

Mesut TARTUK[1], F. Taha NURDAĞ[2], Vedat ACAR[3], Sevtap ERDEM[4], M. Fatih AKAY[5] and Fatih ABUT[6]*

[1]*Comdata Teknoloji ve Müşteri Hizmetleri A.Ş., Turkey, mesut.tartuk@comdatagroup.com*
[2]*Comdata Teknoloji ve Müşteri Hizmetleri A.Ş., Turkey, furkan.nurdag@comdatagroup.com*
[3]*Comdata Teknoloji ve Müşteri Hizmetleri A.Ş., Turkey, vedat.acar@comdatagroup.com*
[4]*Çukurova University, Engineering Faculty, Department of Computer Engineering, Turkey, sevtaperdem10@gmail.com*
[5]*Çukurova University, Engineering Faculty, Department of Computer Engineering, Turkey, mfakay@cu.edu.tr*
[6]*Çukurova University, Engineering Faculty, Department of Computer Engineering, Turkey, fabut@cu.edu.tr*

Abstract

For companies operating in the call center service sector, it is essential to plan and manage call center employees regularly and optimize the costs. Therefore, agent planning needs to be performed in an optimum way in the call center sector. To make customer representative planning, information on the number of incoming calls is needed to forecast call counts. This study aims to forecast the number of calls using the Extreme Gradian Boosting (XGBoost) combined with consecutive and periodic lookback to be able to plan the number of representatives at specified intervals per operation in the call center sector. Models based on Moving Average (MA) have also been developed for comparison purposes. Mean Absolute Error (MAE) has been used to evaluate the performance of forecast models whereas the generalization errors of the models were evaluated using 80/20 split for training and testing. Forecasts were generated in daily format for four different weeks. The results show that XGBoost performs better than MA for all four different weeks and produces predictions within limits of acceptable accuracy.

Keywords: Machine learning, Regression, Forecasting, Call center.

Received:09.05.2022
Accepted:08.06.2022
Published:30.06.2022
**Corresponding author:* Fatih Abut, *PhD*
Çukurova University, Engineering Faculty, Department of Computer Science, Adana, Turkey
E-mail: fabut@cu.edu.tr
Cite this article as: M. Tartuk, F. T. Nurdağ, V. Acar, S. Erdem, M. F. Akay and F. Abut, Forecasting Call Center Arrivals Using XGBoost Combined with Consecutive and Periodic Lookback, *Eastern Anatolian Journal of Science, Vol. 8, Issue 1, 20-25, 2022.*

1. Introduction

Call Centers are interaction centers consisting of software, hardware, human resources, and workflows, where institutions communicate with the people or institutions they are in contact with. It is an inclusive name generally given to structures such as reservation centers, help desks, information lines, and customer relations. The main purpose of a call center for a company is to meet product or information requests from customers. The biggest advantage of call centers is that they increase the efficiency of the transaction depending on the business processes and add a plus to the customer transactions.

Call center managers are faced with multiple operational decision-making tasks. One of the most common tasks is to determine the weekly workforce limit to meet the customers' needs and ensure their satisfaction while keeping the service costs at a minimum level. The first step in producing a weekly schedule is to determine the number of agents that will work at intervals determined by the operation.

Representatives working in call centers are usually paid for the hours they work. However, an insufficient number of representatives to provide service in a busy working day planned in advance causes the call traffic to not be kept up and the waiting times to increase. This directly leads to customer dissatisfaction and complaints. On the other hand, hiring too many representatives for a day with low call traffic causes unnecessary travel, food, and wage expenses for the call center. Therefore, determining the number of customer representatives for the operation is crucial. Information on the number of incoming calls is needed in advance to plan the number of representatives to work at intervals determined based on the operation.

Numerous methods have been used to forecast call arrivals in call centers in the last few years. (Albrecht et al., 2021) introduced the capabilities of Machine Learning (ML) models for forecasting call center log calls regarding forecast accuracy and applicability. Relevant ML approaches and the most commonly used time series models were compared via cross-validation. Historical call center data was examined in (Kanthanathan et al., 2020). The study intended to learn the data trends and then estimate the number of incoming calls for the contact center. Traditional Recurrent Neural Networks (RNN) and their variants Long-Short-Term Memory (LSTM), Gated Repetitive Unit (GRU), and Bidirectional Long-Short-Term Memory-Bi-LSTM methods have been found to be successful in estimation. (Zhang et al., 2021) developed an Autoregressive Integrated Moving Average (ARIMA) model and a Long Short-Term Memory (LSTM) neural network model based on time series used to predict call traffic. (Ballouch et al., 2021) proposed MLP-based and LSTM-based models combined with time lags to forecast the number of call arrivals in a call center. (Leszko, 2020) estimated the expected number of calls from any company in the next 40 days. According to the study results, it was seen that the Seasonal Auto-Regressive Integrated Moving Average (SARIMA) model, which is one of the evaluated ML models, achieved the best result. (Cao et al., 2020) predicted forward call traffic using a holistic method which analyzes and categorizes call traffic data for temporal features. After data preprocessing, an Erlang formula-supported method was developed for extracting time-dependent features to train the prediction model. In (Cao et al. 2019), an effective method was proposed to predict search traffic with multiple forecast results for future periods. In the method, seasonal dependencies are summarized by data analysis, and then different features based on these dependencies are extracted to train the forecast model. (Barrow and Kourentzes 2018) evaluated various univariate Time Series forecasting methods to predict intraday outlier call arrivals. In addition to statistical methods, ANNs were also evaluated. The results show that ANNs accurately predict call center data and can model complex outliers using simple modeling approaches. (Jalal et al., 2016) proposed a model consisting of a combination of Elman and NARX Neural Networks for call duration estimation. The data was divided into training and test sets for model performance review. 80% and 20% of the data were used for training and testing, respectively. As a result, it has been seen that E-NARXNN, which incorporates the advantages of Elman and NARX networks, is more successful than other evaluated models. (Li, 2018) aimed to predict the next peak season call volume using the time series approach. ARIMA and Holt-Winters Exponential Smoothing (HWES) methods were used to estimate call volume's baseline and peak season. The results show that the HWES model outperforms the ARIMA model. In (Motta et al. 2013), a hybrid system using ARIMA and Erlang model for call prediction was introduced. While training the model, day and time parameters were considered. (Kim et al., 2012) forecasted peak call arrivals of rural electric cooperatives call center. They used Gaussian copula to capture the dependence between non-normal distributions. (Rafiq 2017) proposed an agent personalized call prediction method that encodes agent skill information as the prior knowledge for call prediction and distribution. (Moazeni and Andrade 2018) used a data-driven approach to predict an individual customer's call arrival in multichannel customer support centers.

This study aims to forecast the number of calls using the XGBoost method combined with a consecutive and periodic lookback. Models based on MA were also developed for comparison purposes. The MAE has been used for evaluating the performance of the forecast models, whereas the generalization errors of the models were evaluated using 80/20 split for training and testing. Forecasts were generated in daily format for four different weeks. The results show that XGBoost performs better than MA for all four different weeks and produces predictions within limits of acceptable accuracy.

This paper is structured as follows. Section 2 provides information on dataset and methodology. Section 3 presents the results and discussion. Section 4 concludes the paper along with possible future research direction.

2. Dataset Generation and Methodology

This study utilized a data set collected in hourly time intervals obtained from Comdata in Turkey. The dataset includes call counts that arrived at the call center from January 1st, 2018, to October 31st, 2021,

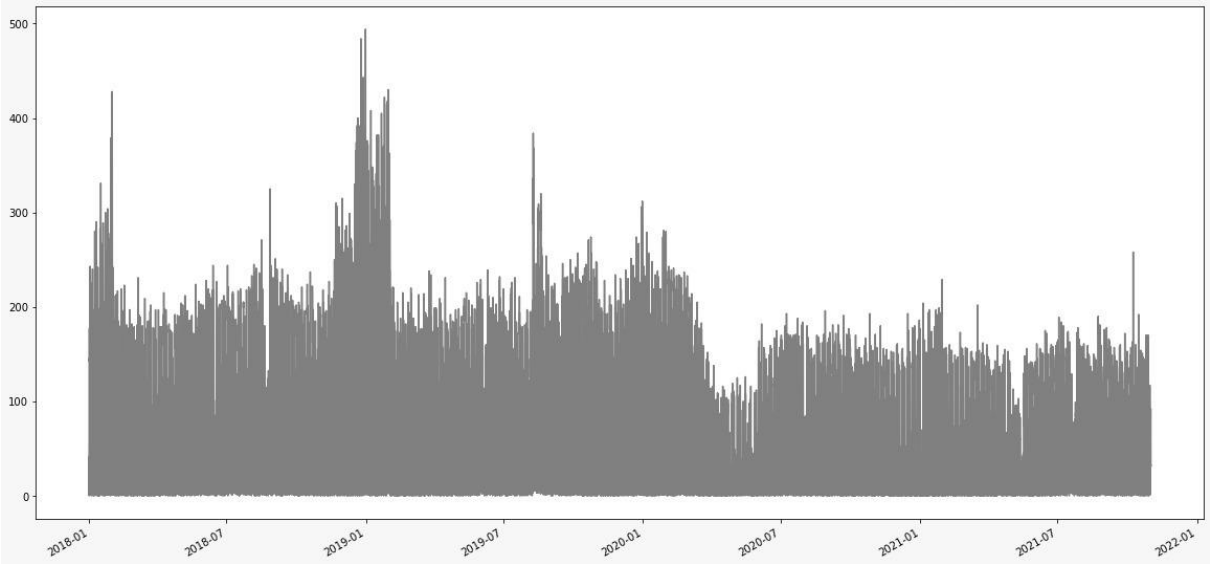

Figure 1: Number of calls on an hourly basis

on an hourly basis. Figure 1 illustrates the number of calls on an hourly basis. The predictor variables are year, month, hour, and weekday and the target variable is the number of call arrivals.

The boosting algorithm creates new weak learners and sequentially combines their predictions to improve the model's overall performance. For any incorrect prediction, larger weights are assigned to misclassified samples and lower ones to correctly classified samples. Weak learner models that perform better have higher weights in the final ensemble model.

Another variation of the boosting algorithms is XGBoost. The most important features of the algorithm are that it can achieve high predictive power, prevent over-learning, manage empty data and perform quickly. Software and hardware optimization techniques have been applied to obtain superior results using fewer resources. XGBoost is considered as one of the best decision tree-based algorithms.

One of the important factors that make the XGBoost algorithm powerful is that the tree structure created tends to minimize the error of the next tree from the previous tree. The important parameters that will affect the successful performance of the XGBoost model are the booster value, the learning rate, the gamma (i.e., minimum split loss), the maximum depth, the minimum number of leaves, lambda (i.e., the parameter that prevents over-learning), and alpha (i.e., the parameter that controls the regulation of the weights).

Consecutive and Periodic Lookback Integration is an algorithmic improvement developed to use the historical data of the target variable to be predicted on the side of supervised learning in the training dataset. Sequential lookback is how much data of the target variable will be taken as a basis for predicting, e.g., how much past sales will be used to estimate future sales. There are two values in periodic lookback. The first value is the number of periods which indicates how many times the operation to be entered into the second value will be performed, e.g., if a daily forecast is to be made, how many Fridays will go back to predict the next day. The second value is calculated according to the period of the series (i.e., weekly: 4, daily: 7, hourly: 7x24, etc.). To summarize, if the values of 2-7 are selected in a dataset in the periodic lookback daily format, this means that one goes back 7 days from the day the training data ended and adds that value to the training set, and repeats this process 2 times. In future forecasting problems, the size of the sequential and periodic historical data to create forecasting models plays an important role.

The performance of the models has been evaluated by calculating the MAE metric, shown in Eq. (1). n is the number of forecasts, A is the actual value, and F is the forecasted value. The

generalization errors of the models were evaluated using 80/20 split for training and testing.

$$\text{MAE} = \frac{1}{n}\sum_{i=1}^{n}|A - F|, \quad (1)$$

3. *Results and Discussion*

The hourly call counts in the fourth week of June, the second week of July, the third week of August, and the second week of September were forecasted, and the rest of the data was used to train the models. According to weekly forecasts, the consecutive and periodic lookback values are 7/8-7, 14/4-7, 7/4-7, and 21/8-7, respectively.

Figure 2 through Figure 5 show MAEs of XGBoost-based models combined with consecutive and periodic lookbacks and MA-based models.

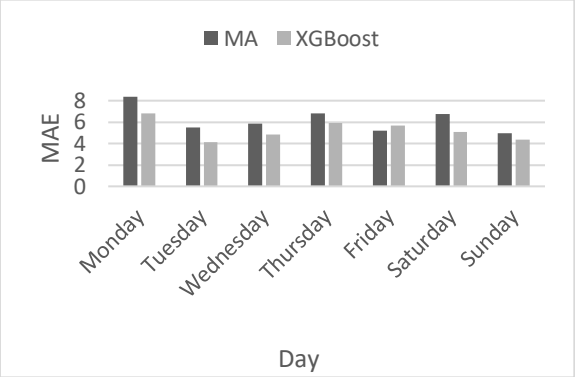

Figure 2. MAEs of forecast models for the fourth week of June using XGBoost and MA

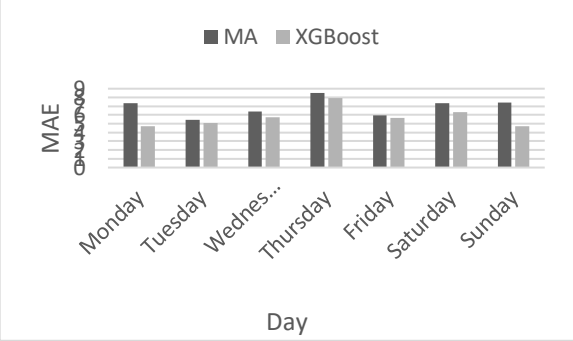

Figure 3. MAEs of forecast models for the second week of July using XGBoost and MA

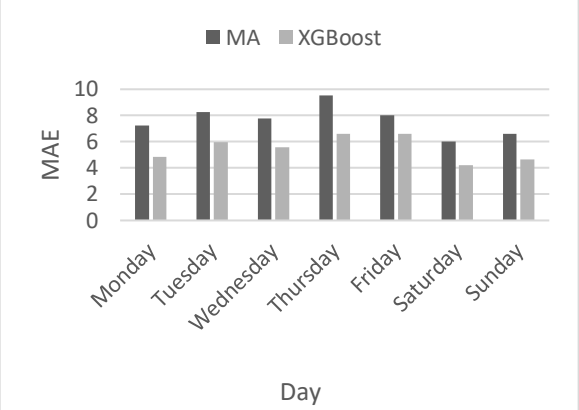

Figure 4. MAEs of forecast models for the third week of August using XGBoost and MA

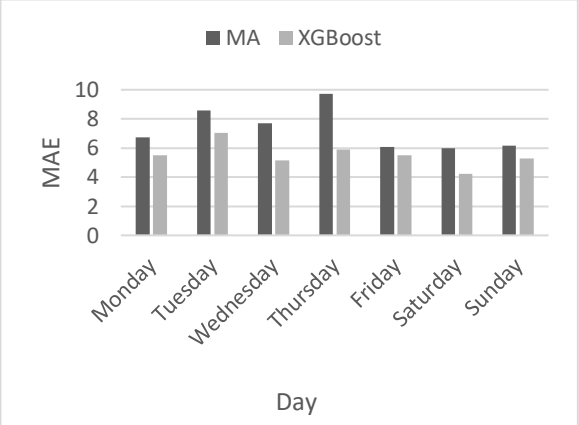

Figure 5. MAEs of forecast models for the second week of September using XGBoost and MA

The results show that

- the MAE values of XGBoost-based forecast models for the fourth week of June change between 4.11 and 8.39, whereas the MAE values of the MA-based models range from 4.95 to 8.39.
- the MAE values of XGBoost-based forecast models for the second week of July change between 4.70 and 7.94, whereas the MAE values of the MA-based models range from 5.55 to 8.50.
- the MAE values of XGBoost-based forecast models for the third week of August change between 4.23 and 6.61, whereas the MAE values of the MA-based models range from 6.00 to 9.54.
- the MAE values of XGBoost-based forecast models for the second week of September change between 4.23 and 7.04, whereas the

MAE values of the MA-based models range from 6.08 to 9.70.

It is clearly seen that the XGBoost-based models consistently outperform the MA-based models in forecasting the call center arrivals. It can be concluded that

- the average MAE value obtained with XGBoost in the fourth week of June is 15.59% lower than that obtained with MA.
- the average MAE value obtained with XGBoost in the second week of July is 16.78% lower than that obtained with MA.
- the average MAE value obtained with XGBoost in the third week of August is 28.01% lower than that obtained with MA.
- the average MAE value obtained with XGBoost in the second week of September is 24.41% lower than that obtained with MA.

4. Conclusion and Future Work

In this study, we proposed XGBoost-based models combined with consecutive and periodic lookback for forecasting the number of call arrivals in call centers. For comparison purposes, models based on MA were also developed. The dataset was created by including call counts that arrived at the call center of Comdata in Turkey from January 1st, 2018, to October 31st, 2021, on an hourly basis. Weekly forecasts have been produced on hourly periods. MAE has been utilized to assess the performance of the forecasting models. Models' generalization errors were evaluated using 80/20 split for training and testing. The results show that XGBoost models combined with consecutive and periodic lookbacks are superior to MA models. We can conclude that XGBoost-based forecasting models can be effectively used for predicting the call arrivals of a call center.

As future research direction, another interesting direction would be extending the existing forecasting models to simultaneously predict different call types, such as call counts related to receiving information about products, campaigns, and solutions to technical problems. Furthermore, quarterly and yearly call arrival forecasting models can be developed to enable long-term capacity planning in call centers.

References

ALBRECHT, T., RAUSCH, T. M., & DERRA, N. D. (2021). Call me maybe: Methods and practical implementation of artificial intelligence in call center arrivals' forecasting. Journal of Business Research, 123, 267-278.

BALLOUCH, M., AKAY, M.F., ERDEM, S., TARTUK, M., NURDAG T.F., YURDAGUL, H.H., "Forecasting Call Center Arrivals Using Machine Learning," Osmaniye Korkut Ata University Journal of Natural and Applied Sciences, vol. 4, no. 1, pp. 96-101, 2021.

BARROW, D., & KOURENTZE, N. (2018). The impact of special days in call arrivals forecasting: A neural network approach to modelling special days. European Journal of Operational Research, 264(3), 967-977.

CAO, B., WU, J., CAO, L., XU, Y., & FAN, J. (2020). Long-term and multi-step ahead call traffic forecasting with temporal features mining. Mobile Networks and Applications, 25(2), 701-712.

CAO, L., MA, K., CAO, B., & FAN, J. (2019). Forecasting long-term call traffic based on seasonal dependencies. In International Conference on Collaborative Computing: Networking, Applications and Worksharing (pp. 231-246). Springer, Cham.

JALAL, M. E., HOSSEINI, M., & KARLSSON, S. (2016). Forecasting incoming call volumes in call centers with recurrent neural networks. Journal of Business Research, 69(11), 4811-4814.

KANTHANATHAN, C., CARTY, G., RAJA, M. A., & RYAN, C. (2020). Recurrent Neural Network based Automated Workload Forecasting in a Contact Center. In 2020 3rd International Conference on Intelligent Sustainable Systems (ICISS) (pp. 1423-1428). IEEE.

KIM, T., KENKEL, P., & BRORSEN, B. W., Forecasting hourly peak call volume for a rural electric cooperative call center. Journal of Forecasting 2012; 31(4), 314-329.

LESZKO, D. (2020). Time series forecasting for a call center in a Warsaw holding company (Doctoral dissertation).

LI, J. (2018). Forecasting and Improving the Call Center Operations-Time Series Approach and Queueing Theory Approach (Doctoral dissertation, UCLA).

MOAZENI, S., AND ANDRADE, R., "A Data-Driven Approach to Predict an Individual Customer's Call Arrival in Multichannel Customer Support Centers," 2018 IEEE

International Congress on Big Data (BigData Congress), San Francisco, CA, 2018, pp. 66-73.

MOTTA, G., BARROERO, T., SACCO, D., & YUO, L. (2013). Forecasting in multi-skill call centers: a multi-agent multi-service (MAMS) approach: research in progress. In 2013 Fifth International Conference on Service Science and Innovation (pp. 223-229). IEEE.

RAFIQ, M., (2017). Using Personalized Model to Predict Traffic Jam in Inbound Call Center. ICST Transactions on Scalable Information Systems. 4. 152101. 10.4108/eai.18-1-2017.152101.

ZHANG, M., SHENG, Y., TIAN, N., LIU, W., WANG, H., ZHU, L., & XU, Q. (2021, April). Research and Application of Traffic Forecasting in Customer Service Center Based on ARIMA Model and LSTM Neural Network Model. In Journal of Physics: Conference Series (Vol. 1881, No. 3, p. 032063). IOP Publishing.

NOTLAR

NOTLAR


AGRI
IBRAHIM CECEN
UNIVERSITY
2007
EASTERN ANATOLIAN JOURNAL OF SCIENCE
2015